

Microfluidic enzyme reactor with immobilized human intestinal microsomes

Duvnjak, Zrinka

Master's thesis / Diplomski rad

2022

Degree Grantor / Ustanova koja je dodijelila akademski / stručni stupanj: **University of Zagreb, Faculty of Pharmacy and Biochemistry / Sveučilište u Zagrebu, Farmaceutsko-biokemijski fakultet**

Permanent link / Trajna poveznica: <https://urn.nsk.hr/urn:nbn:hr:163:782994>

Rights / Prava: [In copyright](#)/[Zaštićeno autorskim pravom.](#)

Download date / Datum preuzimanja: **2025-03-14**



Repository / Repozitorij:

[Repository of Faculty of Pharmacy and Biochemistry University of Zagreb](#)



Zrinka Duvnjak

**Microfluidic Enzyme Reactor with Immobilized
Human Intestinal Microsomes**

MASTER'S THESIS

University of Zagreb, Faculty of Pharmacy and Biochemistry

Zagreb, 2022

This thesis has been submitted to the University of Zagreb, Faculty of Pharmacy and Biochemistry. The experimental work was conducted at the Unit of Pharmaceutical Nanotechnology and Chemical Microsystems, Division of Pharmaceutical Chemistry and Technology, Faculty of Pharmacy, University of Helsinki, under the expert guidance of associate professor Dr Tiina Sikanen and under the supervision of assistant professor Dr Hrvoje Rimac.

Acknowledgements

First and foremost, I would like to thank Tiina for accepting me into her group so nicely, for her guidance, insightful comments and for stepping in every time when needed. Huge thanks also go to Vera, who was sharing her knowledge with me on an everyday basis and who made me aware of so many tiny details which I needed to become truly independent in research. At the same time,

I am very thankful for Vera's friendliness and understanding. I would also like to thank other group members, especially Tea and Iiro K, who were always eager to help, and Kati and Iiro R for also becoming my friends outside of the lab.

Special thanks also go to my friend Matteo, for being my lunch buddy and for listening about my experiments' outcomes day by day.

Veliko hvala i mom drugom mentoru, Hrvoju, koji je uskočio kada je trebalo i u kratkom vremenu me poučio o pisanju znanstvenog rada.

Hvala i svim mojim prijašnjim mentorima bez kojih danas ne bih bila tu gdje jesam te koji su mi povećavali interes za znanost i nove spoznaje.

Posebno sam zahvalna što sam bila dio CPSA-e, gdje sam došla u doticaj s mnogim ljudima koji su mi nesvjesno davali ideje čime bih se sljedeće mogla baviti. Najzahvalnija sam što mi je pružila prvi doticaj s putovanjima i internacionalnim prijateljima. Također sam zahvalna na drugim aktivnostima na fakultetu kao što su odbojka i zbor, što je dodatno obogatilo moje studiranje i krug prijatelja te mogućnostima odlaska na Erasmus, što me je kroz ove godine najviše oblikovalo.

Hvala bratstvu ZΦΣ na svim druženjima, aktivnostima, partijima, učenju s plaže te što su studiranje učinili neizmjerljivo lakšim i zabavnijim, a nikad usamljenim. Hvala Ivanu bez kojeg neki ispiti ne bi bili tako lako položeni.

Neizmjerljivo sam zahvalna svojim najboljim prijateljima s kojima sam uvijek mogla podijeliti sve brige i sretne trenutke – hvala mojim najdražim cimericama Ivi i Heleni te Valentini i Henčel sa Šare, hvala Markecu i bratiću Dariju.

Hvala i prijateljima iz Nove Gradiške, koji su i nakon toliko godina i dalje tu za mene.

Najveće hvala mojoj obitelji – sestri koja mi cijeli život pokazuje "kako se to može", koja je u svim životnim situacijama bila podrška i referentna točka te roditeljima koji su mi sve omogućili i uvijek me podržavali u svim mojim naumima.

Veliko hvala i svima drugima koji su ove godine studiranja učinili lijepima i sretnima!

Table of contents

1. Introduction.....	1
1.1. Microfluidics.....	1
1.1.1. Materials for Microchips Fabrication.....	3
1.1.2. Enzyme Immobilization.....	6
1.2. Intestinal Metabolism.....	10
1.2.1. Relevance.....	10
1.2.2. Factors Affecting Intestinal Metabolism.....	12
1.2.3. Enzyme Inhibition Classification.....	14
2. Aim of the Project.....	16
3. Materials and Methods.....	17
3.1. Materials.....	17
3.2. Microchip Microfabrication.....	19
3.3. Microchip Functionalization and Immobilization of Human Intestinal Microsomes.....	20
3.4. Size and ζ -Potential of Microsomes.....	22
3.5. Model Reactions.....	23
3.6. Implementation of Static Assays.....	25
3.7. Implementation of Flow-Through Assays.....	25
3.8. Quantification of Enzymes Immobilized.....	28
4. Results and Discussion.....	29
4.1. Comparison of HIM and HLM.....	29
4.1.1. Enzyme Activity.....	29
4.1.2. Size and ζ -Potential.....	31
4.2. Optimization of the Immobilization Method.....	31
4.3. Finding Suitable Marker Substrates.....	33
4.3.1. Screening of New Pre-fluorescent CYP3A4 Probes.....	34
4.4. IMER Characterisation.....	35
4.4.1. Enzyme Immobilization Yield.....	35

4.4.2. Enzyme Activity	36
4.4.3. Stability of the Enzyme Activity under Flow-Through Conditions.....	36
4.5. IMER Setup as a Concept for Assessment of Drug-Drug Interactions.....	37
4.5.1. Comparison of Inhibition of CYP3A4 Activity by Ketoconazole in HIM and HLM.....	38
4.5.2. Comparison of BR Transformation in HIM and HLM	40
4.5.3. Inhibition of BR Transformation by CYP1B1 Inhibitors	40
5. Conclusion	46
6. Abbreviation List	47
7. References.....	48
8. Summary/Sažetak	55
9. Attachments	57
9.1. Information About Enzyme Source from the Supplier	57
9.1.1. HIM.....	57
9.1.2. HLM.....	58
Curriculum Vitae	i
Temeljna dokumentacijska kartica	iv
Basic documentation card.....	v

1. INTRODUCTION

1.1. Microfluidics

Microfluidics, in its simplest, is a manipulation of fluids on a micron level. Furthermore, it is considered a technology of manufacturing platforms for fluid manipulation (*e.g.*, microchips), usually small devices containing tunnels and chambers through which fluids flow, but it is also a science that studies behaviours and laws (such as laminar flow) behind fluids flowing through the tunnels on a micron level. The main idea of microfluidics is to create a micro-sized system that will perform operations for which usually a whole lab is needed and, in this way, save reagents, shorten the time needed for performing tasks and exploit merits of flow-through conditions and laminar flow (Whitesides, 2006).

With regards to the interfaces, microfluidics can be classified into three groups: digital, droplet (segmented flow), and continuous flow microfluidics (Figure 1). These groups have significant differences, but all of them have found their application in many stages of pharmaceutical development. Digital microfluidics (Figure 1A), based on the use of electrowetting, offers an open platform for controlled drug synthesis and different biological assays. By using the droplet-based microfluidic approach (Figure 1B), where droplets are formed due to fluids' immiscibility, uniform and complex drug carriers with high encapsulation efficacy can be created, or droplets can be used as small containers for high-throughput screening (Liu *et al.*, 2021).

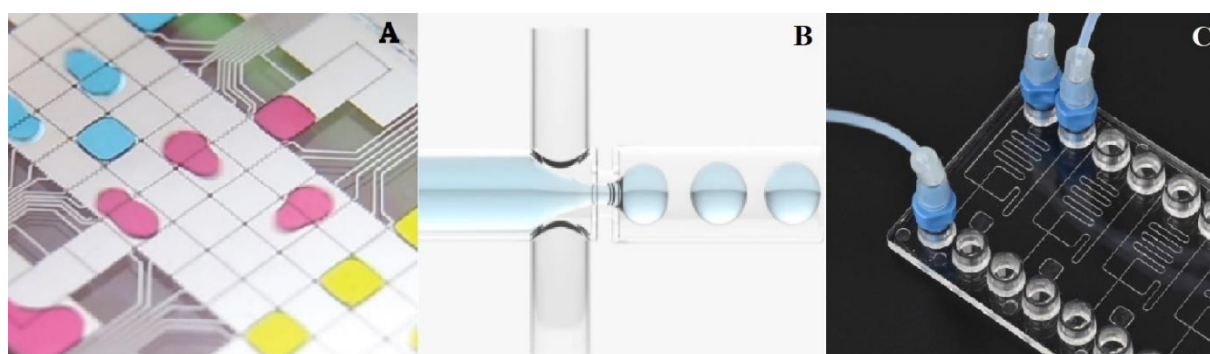


Figure 1. Classification of microfluidics. A) digital microfluidics, B) droplet microfluidics, C) continuous flow microfluidics (photos reproduced with permission from: A: <https://research2reality.com/health-medicine/shrinking-the-lab/> B: <https://www.elfeflow.com> C: https://www.bi-pol.com/microfluidics_chips/).

In all continuous-flow applications, there are no liquid droplets formed, instead the flow is a single miscible phase and usually serves for delivering, mixing, splitting, and taking away substances in a controlled manner. Some applications of continuous-flow microfluidic are organ-on-a-chip, immobilized enzyme microreactor (IMER), micro-total-analysis-system (μ TAS) and lab-on-a-chip (Figure 1C).

Organ-on-a-chip (*e.g.*, liver, kidney, heart, gut, brain) is a biomimetic system which incorporates cell culture, where the chip microenvironment is mimicking the organ microenvironment in the terms of mechanical stimulation and tissue interfaces (Wu *et al.*, 2020).

IMER is a microfluidic device that has immobilized enzymes in its chambers and allows performing enzymatic experiments under flow-through conditions. The most common IMER models incorporate proteolytic enzymes (*e.g.*, trypsin, pepsin) for carrying out on-chip protein digestion, but other enzymes, such as metabolising enzymes, can also be immobilized. The flow rate can be fine-tuned, and its feed composition can be easily modified while performing the experiment, which allows a convenient determination of enzyme kinetic parameters and mechanistic studies of drug-drug interactions. Moreover, there is no product-separation step needed since enzymes (proteins) which disable direct analysis are affixed inside the microchip, so only products and unused substrates/cosubstrates are eluted. Besides, the reactors can be reused, which in addition to miniaturization itself, decreases the cost of the experiments (Nicoli *et al.*, 2008).

μ TAS integrates one or more laboratory functionalities, for instance, microfluidic capillary electrophoresis, and it offers high resolution and sensitivity, low cost, and short analysis time.

Lab-on-a-chip is a microdevice that includes more of the above-mentioned devices, such as coupling organ-on-a-chip or IMER to μ TAS. The aim is integration of many functional elements, such as sample preparation, separation, reactions, continuous monitoring, and detection, to produce truly sample-in/answer-out systems (Patabadige *et al.*, 2016).

Microfluidic devices are characterized by rapid mass and heat transfers, a high surface to volume ratio, low cost due to low consumption of reagents, and controllability. Moreover, the presence of flow-through conditions and laminar flow offers completely new possibilities. Hence, microfluidics has a great potential to change the drug research and development paradigm.

1.1.1. Materials for Microchips Fabrication

A microfluidic chip is a device with a set of micro-channels etched or molded into a material and these micro-structures are made by a process called microfabrication. The earliest microfabrication processes were used in the semiconductor industry, for integration of circuits into silicon. These processes were then taken, adapted, and applied to many other materials (glass, polymers) and fields, one of which is fabrication of microfluidic devices for pharmaceuticals development.

Polymer microfabrication techniques can be divided into two groups: direct machining methods (micromachining and lithography), and replication methods (embossing and casting).

Photolithography is widely used in production of electronic components where it is applied for a direct processing of silicon, which is a final material of electronic components (Becker and Gärtner, 2008). Since in general the highest accuracy and feature resolution is accomplished by lithography (Xia and Whitesides, 1998), photolithography in the microfluidics field is used as an intermediate step, where the structures made in the photolithography process are used as a high-definition mold for polymer replication (Becker and Gärtner, 2008)(Figure 2).

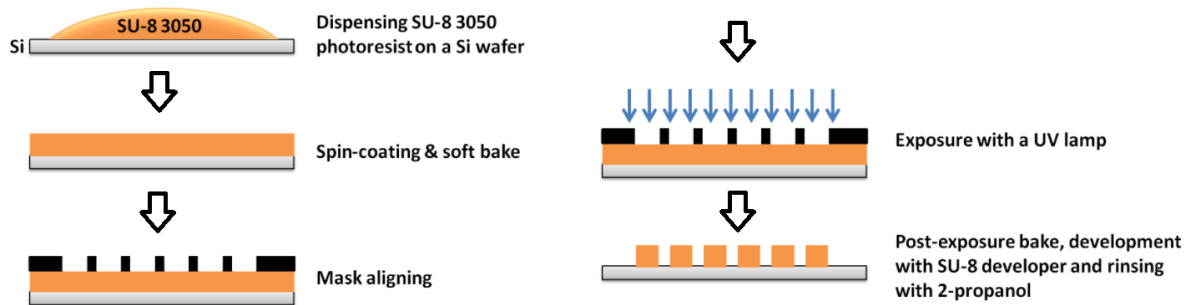


Figure 2. Fabrication of master SU-8 mold by photolithography (adapted from Millionis et al., (2013) with permission of the publisher).

Silicon was the material of choice for integration of circuits due to its semiconductive properties, however it was not very suitable for fabrication of microfluidic devices. Silicon fabrication is costly, it requires use of hazardous chemicals and a clean-room environment, it is not transparent, and its semiconductive properties are inadequate when it comes to microfluidic devices, which require high voltages, *e.g.*, for capillary electrophoresis. On the other hand, it is compatible with organic solvents, it has great surface stability, and allows for high precision machining (Becker and Gärtner, 2008).

Glass is the second material used from the beginning of microchip fabrication due to its good properties, such as stability of surface chemistry and charge, thermal conductivity, solvent compatibility, transparency, high-pressure resistance, hydrophilicity, and its chemical inertness. The reason why glass is not commonly used is complicated and high-cost microfabrication of glass microdevices (Becker and Gärtner, 2008).

Today, the most used microchip materials are polymers, with their lower fabrication cost and a possibility of having various tailored physicochemical, as well as mechanical properties. From the utility point of view, polymers can be classified into three groups: thermoplastic materials, elastomers and thermosets (Becker and Gärtner, 2008).

Thermoplastic materials show a distinct softening phenomenon around the glass transition temperature (T_g). However, there is no curing at elevated temperatures so the material can be reshaped many times. Most polymers around us are thermoplastics, such as acrylic, polyester, polypropylene, polystyrene, nylon, and teflon (Becker and Gärtner, 2008).

In elastomers, molecular chains are much longer compared to the other types of polymers and there is no chemical interaction between them. Instead, they are only physically entangled. Elastomers can be stretched, but they always return to their original form after the removal of the external force. For microfluidics, an important elastomer example is polydimethylsiloxane (PDMS) (Figure 3B). Due to its optical transparency, cell compatibility, oxygen permeability, ease of (adhesive) bonding, and affordability, PDMS is the most favoured polymer for organ-on-a-chip applications. On the other hand, PDMS has certain drawbacks, such as swelling upon organic solvent exposure or rapidly becoming hydrophobic, which can cause adsorption of lipophilic molecules and which is especially problematic when working with pharmaceuticals that are mostly lipophilic. Hydrophobic nature is a major downside of PDMS and the reason why alternatives to PDMS are needed. Elastomeric properties of PDMS are inadequate for many commercial products, which need mechanical strength, but the same properties are useful when PDMS has the role of a mold, because detachment of PDMS from rigid structures is easy. (Ren *et al.*, 2013).

Thermosets are materials which can be liquid at room temperature, but at a sufficient dose of radiation, they start to cure (molecular polymer chains start to cross-link). This process is irreversible, so thermosets cannot be reshaped once they are cured. In microfluidics, thermosets are used as lithography resist materials (Figure 2) (Becker and Gärtner, 2008). One of the commonly used thermosets in microfluidic applications is SU-8 – a negative photoresist (parts

that were exposed to radiation polymerize), which contains eight epoxy groups, which are available for acidic-driven cross-linking (Figure 3A). It was primarily developed for manufacturing of high microstructures, because previously used low-viscosity materials only allowed production of microstructures from 0.5 to 3.0 μm in height, which was not sufficient for microfluidic devices. Its advantages are high mechanical, thermal, and chemical stability (Abgrall *et al.*, 2007).

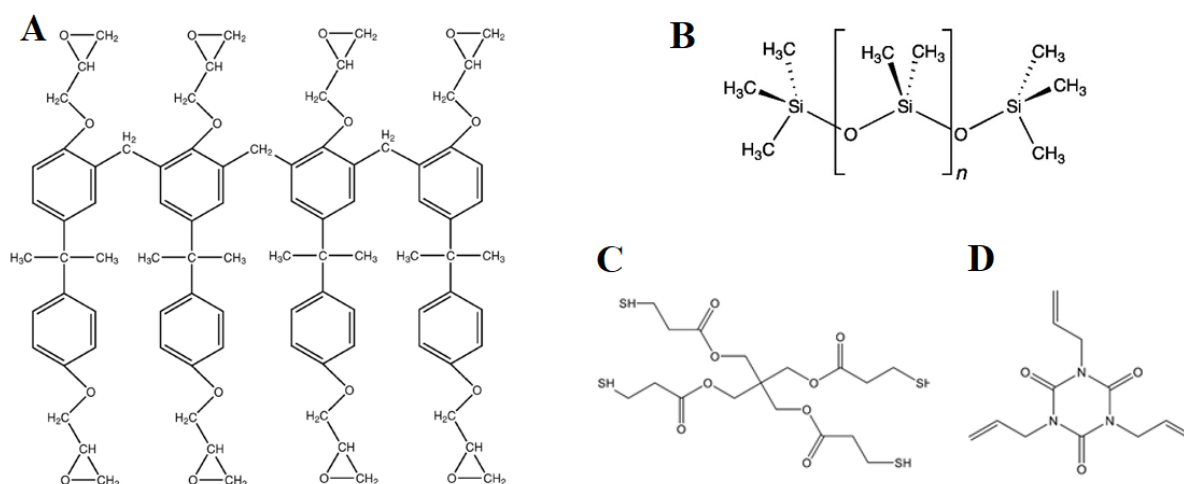


Figure 3. Structures of monomers (polymers) used in this work. A) SU-8 monomer, B) PDMS polymer, C) tetrathiol monomer, D) triallyl monomer.

Thiol-enes are a group of thermoset polymers composed of two monomers, the first containing at least two thiol groups, and the second containing at least two allyl groups (Figure 3C and 3D). The polymerization reaction is an addition reaction between the thiol and allyl groups and belongs to a group of “click-reactions” due to its high yield, velocity, and specificity. This reaction can be started by a photoinitiator or simply by low-wavelength radiation without a photoinitiator. Omitting a photoinitiator allows leaving some thiol and allyl groups free, both in the bulk and on the surface, while by using a photoinitiator almost all functional groups react (Carlborg *et al.*, 2011). As the reaction progresses, a liquid mixture of polymers transforms into a solid polymer in a short time. When thiol and allyl monomers are mixed in a 1 : 1 ratio of thiol and allyl groups (*e.g.*, 3n of tetrathiol and 4n of triallyl monomers), the polymers formed are called stoichiometric thiol-enes. One considerable advantage of thiol-enes is the possibility of directly creating a functionalized surface by mixing polymers in off-stoichiometric ratio with a consequence of having thiol or allyl functional groups in excess (*e.g.*, mixing 1n of tetrathiol and 1n of triallyl monomers results in an excess of thiol functional groups), both in the bulk and

on the surface. This type of thiol-enes is called off-stoichiometric-thiol-ene (OSTE). Besides the above-mentioned, other advantages of thiol-enes are their transparency in near-UV to visible range, low permeability to organic solvents, and low polymerization shrinkage stress (Carlborg *et al.*, 2011).

An important consideration for material selection in all sorts of enclosed microfluidic devices is a possibility of bonding parts together. Bonding of two parts of off-stoichiometric-thiol-enes with an excess of different functional groups is straightforward because two parts would form numerous covalent bonds. However, the surface inside the microchannel would not be uniform since one side of the microchannel surface would have an excess of thiol (allyl) groups and other three sides would have excess of allyl (thiol) groups. By omitting a photoinitiator from the reaction and allowing residual presence of both thiol and allyl groups, two parts with the same composition (OSTE with an excess of the same functional groups) can be bonded together *via* heating, lamination, and exposure to radiation, and in this way preserve uniformity of the microchannel surface. (Sikanen *et al.*, 2013).

Hydrogels, which resemble extracellular matrix due to their permeability and hydrophilicity, are a perfect material for embedding cells. By creating microchannels in the hydrogel, delivery of cells or nutrients is allowed. Microchannels can be made by direct writing methods or by creating a hydrophobic mold and then allowing gelation (Ren *et al.*, 2013).

Paper is the cheapest of all materials used for microfabrication. When certain areas of a paper device are made hydrophobic, the aqueous solution applied to the paper device will be precisely guided through the hydrophilic region by the capillary effect. These channels can be made by lithographic methods – applying a hydrophobic polymer to the whole paper and then removing it from the microchannel parts (dissolving it) or printing it directly in the desired shape. In addition, paper has some other advantages, such as a large surface-to-volume ratio, filtering properties, with microchannels also showing capillary wicking properties. Paper as a material is promising in portable, low cost bioassays, but it still has many limitations. (Ren *et al.*, 2013)

1.1.2. Enzyme Immobilization

Enzyme immobilization is a process of entrapping enzymes in insoluble matrix, while at the same time preserving their catalytic activity. In comparison to free enzymes in solution, immobilized enzymes are more robust and more resistant to changes in the environment. More importantly, using systems with immobilized enzymes allows enzyme reuse, continuous

conduction of enzymatic processes, rapid reaction termination, and easy recovery of enzymes and products. This is why enzyme immobilization has found its application in many industries: bioremediation, environmental monitoring, biotransformation, food industry, textile industry, detergent industry, pharmaceutical industry, diagnostics, etc. (Hassan *et al.*, 2019).

Both membrane bound and soluble enzymes can be immobilized. Membrane bound enzymes are located in the smooth endoplasmic reticulum *e.g.*, cytochrome P450 (CYP), and UDP-glucuronosyltransferase (UGT). Soluble enzymes are those located in cytosol, such as most proteolytic enzymes or sulfotransferases (SULTs) among metabolising enzymes.

For enzyme immobilization, recombinant enzymes or microsomes are used. Microsomes consist of vesicles prepared from the smooth endoplasmic reticulum (ER) of cells by differential centrifugation – hepatocytes for preparation of human liver microsomes (HLM) or enterocytes for preparation of human intestinal microsomes (HIM). Due to microsomes relative affordability, availability, and acceptable *in vivo* resemblance, they are considered the industry standard model for pre-clinical metabolic profiling and drug interaction studies. Microsomes contain only enzymes present in the ER, however these enzymes conduct the majority of human drug metabolism (Figure 4) (Brandon *et al.*, 2003).

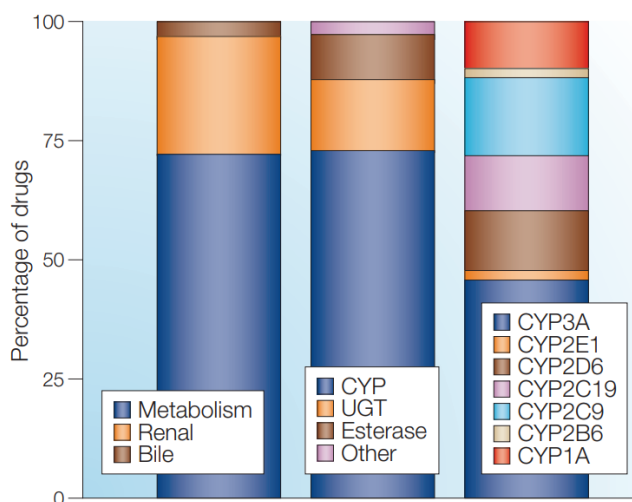


Figure 4. Elimination routes of the top 200 most prescribed drugs in 2002. The first column represents total drug clearance, the second column represents clearance by metabolism and the third column represents CYP-mediated clearance (reproduced from Wienkers and Heath (2005) with permission of the publisher).

For assays where substrates are transformed to metabolites by other enzymatic systems not present in the ER, microsomes cannot be used. Recombinant enzymes can also be both soluble

and membrane bound, but they are expressed in a foreign species, based on transfected human genes. By immobilizing microsomes, different membrane bound enzymes are bound, while by immobilizing recombinant enzymes, only enzymes of choice can be present.

Another important consideration are other parts of enzymatic systems needed for enzymatic function, such as P450 oxidoreductase (POR) or cytochrome b₅, which are responsible for CYP reduction power (electron) supply. These systems need to be embedded in the membrane close to the CYP itself for the whole system to function (Coleman, 2010), which is the case in using microsomes as an enzyme source.

Success of enzyme immobilization can be described as immobilization yield (percentage of enzymes immobilized), immobilization efficiency (percentage of active immobilized enzymes from all enzymes immobilized), and activity recovery, which includes both of the above (immobilization yield multiplied by immobilization efficiency) and gives an idea of total enzyme immobilization successfulness (Sheldon and van Pelt, 2013).

Immobilization approaches can be classified into three main categories: support-binding (binding to a carrier), entrapment (encapsulation), and cross-linking (Figure 5).

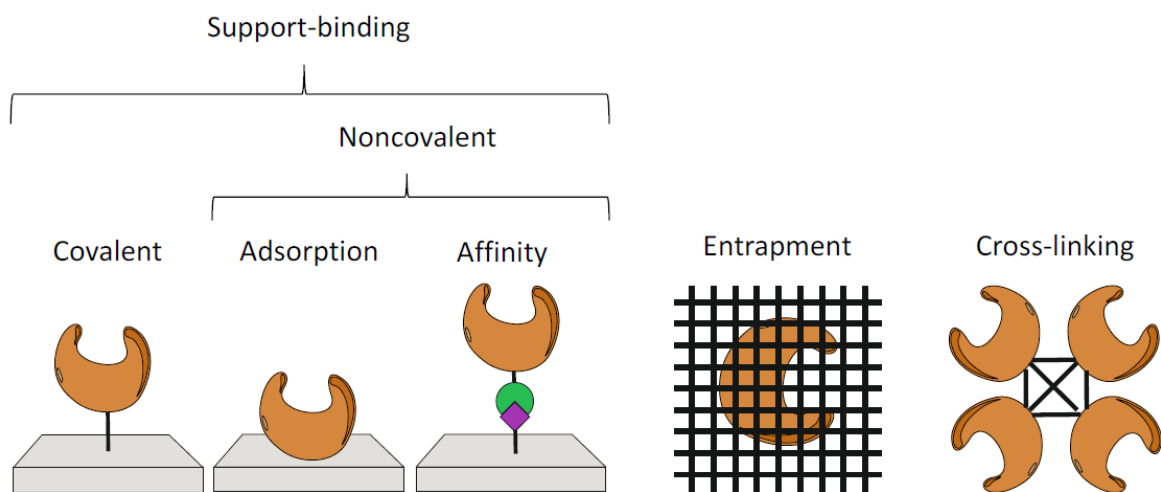


Figure 5. Immobilization strategies (reproduced from Kiiski Iiro (2021) with permission of the author).

Using support-binding approach, enzymes are bound to the support (carrier) *via* strong covalent or ionic interactions, or *via* numerous van der Waals interactions. Enzymes can be bound directly to the microreactor or the microreactor can be filled with carriers to which enzymes are bound (Datta *et al.*, 2013). In contrast to the strong interactions between enzymes and support

in support-binding approach, entrapment suggest that enzymes are physically entrapped in a polymer network, even though chemical interaction is also often present. Entrapment generally requires synthesis of a polymeric matrix in the presence of the enzyme, while in support-binding the support is prefabricated (Sheldon and van Pelt, 2013). Important consideration of entrapment and binding to a carrier is a carrier (support) material. An ideal matrix must encompass characteristics like inertness, physical strength, stability, regenerability, ability to increase enzyme specificity/activity and reduce product inhibition, nonspecific adsorption, and microbial contamination. The support (carrier) can be a synthetic organic polymer, a biopolymer or an inorganic polymer (Datta *et al.*, 2013). In contrast, cross-linking is a support-free approach. In this method enzymes are cross-linked with each other to prepare a large three-dimensional complex molecule using a poly-functional reagent, such as glutaraldehyde. This approach offers clear advantages: highly concentrated enzyme activity in the catalyst, high stability and low production costs owing to the exclusion of an additional (expensive) carrier (Hassan *et al.*, 2019).

The main problems with different immobilization strategies are i) loss of enzyme activity due to enzyme modifications or due to steric reasons and ii) washing off enzymes from the microchip. Washing problems are usually present in non-covalent attachment due to their low binding energies, especially at elevated temperatures and when organic solvents are used. However, a type of non-covalent attachment to the surface, affinity binding, offers strong binding, similar to covalently attached enzymes, but without compromising enzyme activity (Sheldon and van Pelt, 2013).

Recently, HLM was immobilized to microchip by a new method based on the strong and specific streptavidin-biotin interaction (Kiiski *et al.*, 2019). Microchip surface was first functionalized with biotin and then with streptavidin. Microsomes were tagged with biotin by fusion of microsomes and biotinylated fusogenic liposomes. Presence of a biotin-tag within microsomes and streptavidin-functionalized surface of microchips allowed immobilization of microsomes to the microchip by a streptavidin-biotin interaction. Fusion of vesicles is a gentle process and it is facilitated due to low liposome size and opposite surface charges of microsomes and biotinylated liposomes. The biotin tag is added to the membrane, and not at to the protein structure as in other works, so it is located far away from the CYP active site and consequently the active site is reachable by the substrate. As a result, immobilization did not affect enzyme activity. Immobilized enzymes kept their catalytic activity for at least 15 days (Kiiski *et al.*, 2019). In addition, it was shown that UGT isoforms also retain their activity

(Kiiski *et al.*, 2021). Therefore, this immobilization method provides a tool for studying membrane-bound enzymes on solid supports.

1.2. Intestinal Metabolism

By metabolizing xenobiotics, metabolic enzymes make them more hydrophilic, and in this way, they disable drug reabsorption in renal collecting tubules and allow elimination *via* urine. (Coleman, 2010).

Metabolism of drugs mostly leads to a loss of pharmacological activity, while in some exceptions the metabolites can still be pharmacologically active. On the other hand, in some cases, metabolism toxifies substrates into metabolites that can destroy cellular structures. (Bentley *et al.*, 1977).

Liver, having the highest levels of xenobiotic-metabolizing enzymes, is the main organ responsible for drug metabolism and clearance of xenobiotics. Other metabolically active organs in the body, but with much lower xenobiotic-metabolizing enzyme expression, are small intestine, kidneys, lungs, brain, and skin, all having different enzyme expression. Due to their position between external and internal environment, metabolism in skin, respiratory tract, and gastrointestinal tract primarily serve to defend the body from potentially toxic molecules entering the body, whereas the role of hepatic metabolism is primarily to eliminate xenobiotics and endogenous substances from the body (Gundert-Remy *et al.*, 2014).

1.2.1. Relevance

To reach its site of action, an orally administered drug needs to enter systemic circulation, but the fraction reaching it is often rather low. This is due to limitations in drug absorption in the gut, efflux of the drug from the gut wall, metabolism in the gut wall, and finally metabolism in the liver. This process is termed “the first pass” (Figure 6), and therefore, oral bioavailability of a drug is oftentimes significantly lower than its intravenous bioavailability. Since the small intestine is the first exposure site of xenobiotics to a metabolic system and due to its large surface area for absorption, and consequently metabolism, intestinal metabolism can play an important role in the first pass effect. (Coleman, 2010).

For some drugs, intestinal metabolism is clinically relevant, especially for CYP3A substrates such as cyclosporin, midazolam, tacrolimus, nifedipine, felodipine, and verapamil. (Dressman and Thelen, 2009).

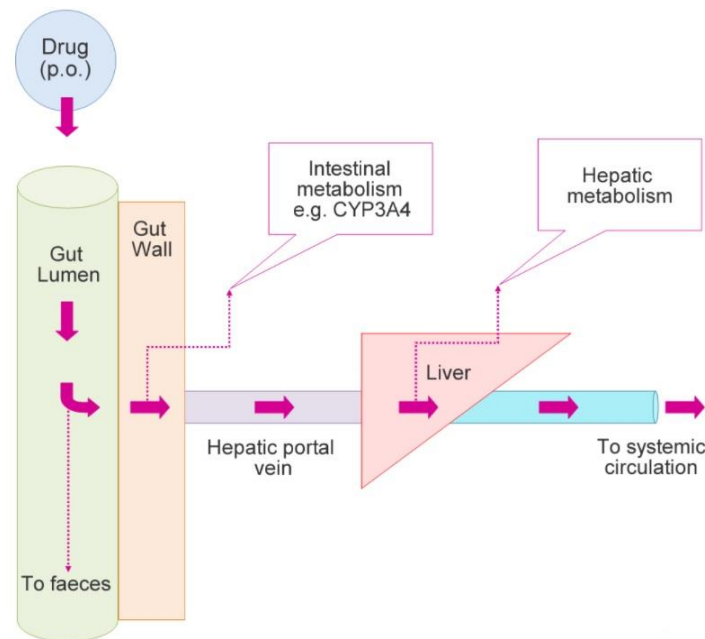


Figure 6. First pass effect (reproduced from: <https://www.knowledgedose.com/drugs-undergoing-extensive-first-pass-metabolism/>).

During drug development, pharmaceutical industry is obligated to determine drug-drug interaction (DDI) potential of a new drug candidate. First, *in vitro* studies are performed, and then if the results are showing potential for DDI, the scope of DDIs in human body is predicted using computational models, such as static models or physiologically based pharmacokinetic (PBPK) models. The area under the curve ratio (AUCR) of a substrate (midazolam and testosterone for CYP3A) with and without the perpetrator (a new drug candidate) is determined. A value of AUCR between 0,8 and 1,25 represents no DDI, and for those candidates with AUCR value outside this interval, clinical DDI studies are needed (EMA, 2012; US Food and Drug Administration, 2020).

One of the reasons behind the importance of intestinal metabolism lies in drug concentrations achieved in cells responsible for drug metabolism, where the drug concentration in enterocytes is higher than the concentration achieved in hepatocytes. This effect is important for weak perpetrators, which obtain AUCRs around 0,8 or 1,25, which are cut-off values. Therefore, intestinal metabolism is needed to obtain accurate results to decide whether clinical DDI studies

are needed or not. Figure 7 shows the importance of intestinal CYP3A metabolism (the gut curve contributes more to the total curve) when the inhibitor is weak (the left part of the left plot – high K_i , low $1/K_i$) and when the inhibitor dose is low (the left part of the right plot) (Yamada *et al.*, 2020). When the inhibitor is strong, intestinal metabolism is completely inhibited, it reaches a plateau, therefore the reciprocal of intestinal availability can be used as a magnitude of DDIs in the intestine, and liver interactions are observed (Galetin, Gertz and Houston, 2008). With consideration of DDIs in the intestine, models more accurately predict if clinical studies are needed, which saves pharmaceutical industry both time and money (Yamada *et al.*, 2020).

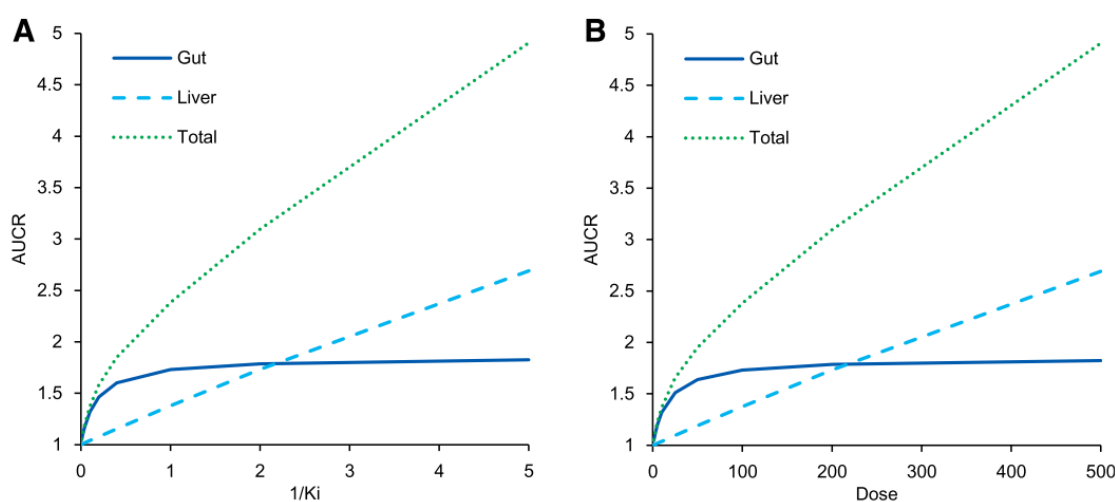


Figure 7. Relationship between midazolam AUCR and K_i with a fixed dose [100 mg, (A)] or doses with fixed K_i [1 mM, (B)] in static model analysis using virtual compounds (reproduced from Yamada *et al.*, (2020) with permission of the publisher).

1.2.2. Factors Affecting Intestinal Metabolism

Activities of metabolizing enzymes in the human intestine are not yet fully characterised. Similar to HLM, CYP3A is the most abundant enzyme found in microsomes prepared from mucosal scrapings of duodenal/jejunal portions, with content of 50 pmol/mg (82% of all enzymes detected). The second most abundant CYP enzyme is CYP2C9, comprising 14% of all enzymes detected. Other CYP enzymes detected were CYP2C19 (2%), CYP2J2 (1,4%) and CYP2D6 (0,7%) (Figure 8) (Paine *et al.*, 2006). Other detected CYP enzymes were CYP1A, CYP2S1, CYP4F12, but their contribution to total metabolism is not high (Dressman and Thelen, 2009). CYP1B1's mRNA was detected in some intestine samples, but the enzyme itself was not (Zhang Q *et al.*, 1999).

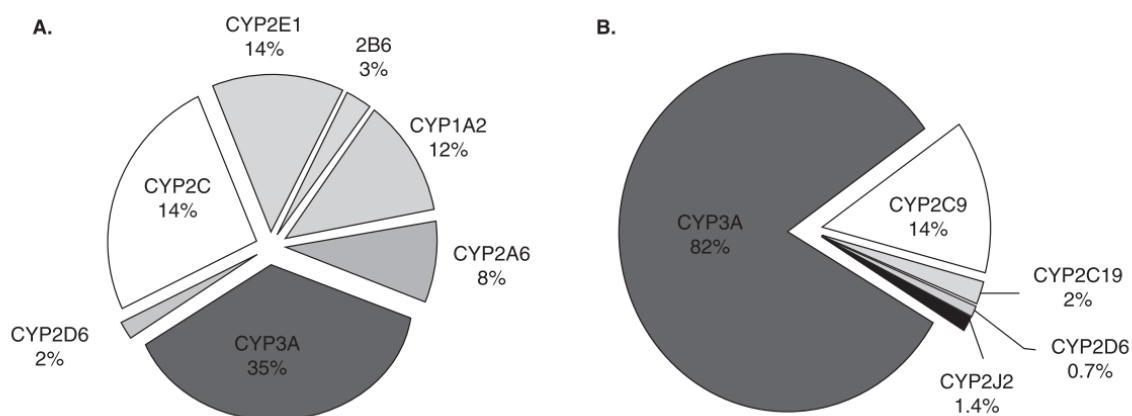


Figure 8. Cytochrome P450 abundance. A) in human liver and B) small intestine (reproduced from Galetin, Gertz and Houston (2008) with permission of the publisher).

The most abundant phase II metabolism enzymes are UGT1A isoforms in the following order: UGT1A7, UGT1A1, UGT1A9, UGT1A8, UGT1A4, UGT1A10, UGT1A6 (Fisher *et al.*, 2001; Harbourt *et al.*, 2012). Another group of phase II enzymes found in human intestine are SULT, where the SULT1B1 enzyme is the most abundant one, followed by SULT1A3, SULT1A1, SULT1E1, SULT2A1 (Riches *et al.*, 2009).

Transporters, considered as the phase III of metabolism, play an important role in bioavailability and elimination *via* active drug transport, but they will not be further discussed in this work.

Apart from the content of the enzyme of interest in enterocytes, the rate of gut wall extraction also depends on the substrate concentration that is affected by other factors, such as absorption, mucosal blood flow and protein binding. Drugs can cross the intestinal epithelium in different manners: passive transcellular diffusion, carrier-mediated pathway, endocytosis, and paracellular pathway. This is important to keep in mind since drugs crossing the intestinal epithelium paracellularly will not be metabolized by intracellular enzymes. When using blood flow for estimation of the intestinal metabolism rate, mucosal but not total intestinal or portal vein blood flow should be considered, since the epithelial layer is supplied with oxygen and nutrients only by mucosal blood flow. In this way, mucosal blood flow affects residence time of a drug in enterocytes, and hence, the time during which a drug is exposed to intracellular metabolizing enzymes. To be transformed by an enzyme, a substrate cannot be bound to plasma proteins. However, the impact of plasma protein binding on the extent of intestinal metabolism should be further investigated (Dressman and Thelen, 2009).

1.2.3. Enzyme Inhibition Classification

Enzyme inhibition is one cause of DDIs and adverse effects of some drugs, therefore it is important to know the type and inhibition parameters of each drug. In the terms of inhibitor's binding site, enzyme inhibition can be classified as competitive, non-competitive, uncompetitive, or mixed inhibition, the latter being a combination of those previously mentioned. The type of inhibition can be determined by making a Lineweaver – Burk plot with and without the inhibitor to conclude which variables are changing: V_{max} (the reaction rate when the enzyme is fully saturated by a substrate), K_m (the concentration of a substrate which permits the enzyme to achieve half V_{max} – a measure of substrate's affinity towards enzyme), or both (Coleman, 2010).

From the effect point of view, inhibitors can be divided to reversible and irreversible inhibitors. Competitive, non-competitive, and uncompetitive inhibitors are usually reversible, while time-dependent inhibitors are mostly irreversible, which means they covalently bind to the enzyme and, thereby, destroy it. Irreversible inhibitors are quite problematic since, in order to recover the metabolic pathway, new enzymes must be synthesized (Coleman, 2010).

Competitive inhibition is the simplest form of enzyme inhibition, and very common in CYPs since it is usually a part of the endogenous feedback control mechanism on product formation. Competitive inhibitors are similar to substrates (drugs) in structure and have a similar affinity for CYP active sites. A substrate is normally transformed by a CYP enzyme to more hydrophilic molecules, which then have a reduced affinity for the active site, so they diffuse elsewhere. An inhibitor, on the other hand, is not metabolized to a more hydrophilic molecule, so it continues to detach and attach to the CYP active site. This process is governed by the law of mass action, which means that whichever compound is in higher concentration, a drug or an inhibitor, will occupy the CYP active site. Drug concentration must be increased to overcome the inhibitor. Effectively, in the presence of an inhibitor, K_m value of a drug toward enzyme increases and the affinity of the drug towards the enzyme decreases, while V_{max} remains unchanged. Important examples of competitive inhibition are azoles, antifungal agents. It is not surprising that they are strong CYP inhibitors since their mechanism of action is inhibition of lanosterol alpha-C14-demethylase, and all CYP systems in the living world originate from the same bacterial source (Coleman, 2010).

In non-competitive inhibition, inhibitor binds not to the active site, but to a different, allosteric site. Binding to an allosteric site triggers a change in enzyme conformation so the enzyme is

less likely to bind a substrate (drug) and transform it. The Lineweaver – Burk plot will show a decrease in V_{\max} (enzyme cannot run at maximal rate), but K_m does not change (affinity of the substrate for the active site is unchanged). Many drugs are non-competitive inhibitors, but it is still not completely clear where their allosteric sites are.

Uncompetitive inhibition is a rare type of enzyme inhibition where inhibitor binds to the enzyme-substrate complex. This binding causes an increase in substrate affinity towards the enzyme (a decrease in K_m), but this complex is not functional, so V_m also decreases.

Another type of inhibition, outside of above-mentioned classification based on binding site, is mechanism-based inhibition. In this type of inhibition, an inhibitor first acts as a substrate, it starts the CYP machinery, a metabolite is formed which then inhibits the enzyme. Mechanism-based inhibitors mostly occupy enzyme active site, but they can also occupy allosteric site *e.g.*, macrolide antibiotics (they are sometimes also classified as non-competitive inhibitors). These inhibitors differ in potency, ranging from inhibitors with a delayed release to inhibitors which terminate enzyme activity irreversibly by covalently binding to the active site of the enzyme. Mechanism-based inhibition can be detected by performing two parallel experiments: one in which enzymes are preincubated with an inhibitor and a cofactor (NADPH), and the other without a cofactor (NADPH) during preincubation, so the CYP cycle cannot be initiated. Detecting the amount of metabolite formed from the substrate, the IC_{50} (half maximal inhibitory concentration) shift can be observed. Some clinically important groups of mechanism-based inhibitors are macrolides, HIV protease inhibitors, SSRIs, diltiazem, verapamil, tamoxifen, irinotecan and grapefruit juice (Coleman, 2010).

2. AIM OF THE PROJECT

By performing conventional enzymatic assays, great amounts of expensive cofactors and enzymes are used. Moreover, for determination of some inhibition parameters, such as inhibition mechanism, numerous assays need to be performed. In addition, before metabolite detection and quantification, an enzyme separation step is required. This altogether results in high financial and time expenses.

Additionally, importance of extrahepatic metabolism is becoming more and more relevant in drug research and development, especially when it comes to drug-drug interactions of weak perpetrators.

With the need of building a more convenient and more affordable platform for intestinal drug metabolism research with solved above-mentioned flaws of conventional assays, and the platform which will better imitate conditions in the human body by incorporating flow-through conditions, the aim of this study is:

- I. development of first of its kind enzyme microreactor with immobilized human-derived intestinal microsomes
- II. characterization and optimization of enzyme microreactor performance in terms of enzyme immobilization yield, stability of enzyme activity under flow-through conditions, and preserved activity of CYP and UGT enzymes
- III. validation of flow-through microreactor concept for assessment of drug metabolism research and of drug-drug interactions in the intestine.

3. MATERIALS AND METHODS

3.1. Materials

All chemicals used in this study were of analytical grade unless otherwise noted. Materials used are separated into four tables (Table 1 – Table 4), suggesting their function. In addition to instruments and equipment mentioned in the following tables, some other standard laboratory equipment was also used.

Table 1. Microfabrication materials.

Chemical / material / instrument	Manufacturer/supplier
SU-8 master	In-house fabrication
Sylgard 184 base elastomer and curing agent	Down Corning Corporation, Midland, MI
1,3,5-triallyl-1,3,5-triazine-2,4,6(1H,3H,5H)-trione ($\geq 98.0\%$) (triallyl)	Sigma-Aldrich, Saint Louis, MO
Pentaerythritoltetrakis(3-mercaptopropionate) ($\geq 95.0\%$) (tetrathiol)	Sigma-Aldrich, Saint Louis, MO or Bruno Bock, Marscacht, Germany
Dymax 5000-EC series UV flood exposure lamp	Dymax Corporation, Torrington, CT
Hot plate	Torrey Pines

Table 2. Materials used for microchips functionalization and enzyme immobilization.

Chemical / material / instrument	Manufacturer/supplier
1,2-dioleoyl-3-trimethylammonium-propane (chloride salt) (DOTAP)	Avanti Polar Lipids, Alabaster, AL
1,2-dioleoyl-sn-glycero-3-phosphoethanolamine (DOPE)	Avanti Polar Lipids, Alabaster, AL
1,2-dioleoyl-sn-glycero-3-phosphoethanolamine-N-(cap biotinyl)(sodium salt) (biotin-cap-DOPE)	Avanti Polar Lipids, Alabaster, AL
1,2-dioleoyl-sn-glycero-3-phosphoethanolamine-N-(lissamine rhodamine B sulfonyl) (ammonium salt) (lissamine rhodamine B-DOPE)	Avanti Polar Lipids, Alabaster, AL
Chloroform	Sigma-Aldrich, Steinheim, Germany
Biotin-PEG4-alkyne	Sigma-Aldrich, Steinheim, Germany
Ethylene glycol	Sigma-Aldrich, Steinheim, Germany
Streptavidin (Alexa Fluor® 488 conjugate)	Life Technologies, Eugene, OR
Pierce™ BCA Protein Assay Kit	Thermo Fischer Scientific, Rockford, IL
Extruder	Avanti Polar Lipids
UV lamp	made in-house
Zetasizer Nano ZS	Malvern, Worcestershire, UK
Zetasizer APS	Malvern, Worcestershire, UK

Table 3. Materials used for performing flow-through experiments.

Chemical / material / instrument	Manufacturer/supplier
11 Elite Syringe pump	Harvard Apparatus, Holliston, MA
Syringes, 1mL	SGE
Hot plate	Labotect
CMA 470 refrigerated microfraction collector	CMA Microdialysis AB, Kista, Sweden
Chip holders	made in-house
Tubing system	made in-house

Table 4. Materials used for carrying out model reactions.

Chemical / material / instrument	Manufacturer/supplier
Water (milli-Q)	Millipore, Molsheim, France
Tris(hydroxymethyl)amino-methane (Trizma® base)	Sigma-Aldrich, Steinheim, Germany
0,01 M phosphate buffered saline (PBS), pH=7,4	Sigma-Aldrich, Steinheim, Germany
Potassium phosphate dibasic anhydrous	Sigma-Aldrich, Steinheim, Germany
Potassium phosphate monobasic	Sigma-Aldrich, Steinheim, Germany
Human liver microsomes (HLM)*	Corning, Wiesbaden, Germany
Human intestinal microsomes (HIM)*	Corning, Wiesbaden, Germany
8-hydroxyquinoline	Sigma-Aldrich, Steinheim, Germany
8-hydroxyquinoline-glucuronide	Sigma-Aldrich, Steinheim, Germany
Perchloric acid	Riedel-de Haën, Seelze, Germany
Uridine 5'-diphosphoglucuronic acid trisodium salt (UDPGA)	Sigma-Aldrich, Steinheim, Germany
β -nicotinamide adenine dinucleotide 2'-phosphate reduced tetrasodium salt hydrate (NADPH)	Sigma-Aldrich, Steinheim, Germany
7-benzyloxyresorufin	Sigma-Aldrich, Steinheim, Germany
Resorufin	Sigma-Aldrich, Steinheim, Germany
Sodium hydroxide	Sigma-Aldrich, Steinheim, Germany
P450-Glo CYP3A4 Assay with Luciferin-IPA	Promega, Madison, WI
Ketoconazole	Sigma-Aldrich, Steinheim, Germany
Paclitaxel	Toronto Research Chemicals, Ontario, Canada
Dimethyl sulfoxide	Sigma-Aldrich, Steinheim, Germany
Acetonitrile	Sigma-Aldrich, Steinheim, Germany
Methanol	Sigma-Aldrich, Steinheim, Germany
Varioskan™ multimode microplate reader	Thermo Fisher Scientific, Vantaa, Finland

*details about microsomes used can be found in the chapter 9.1.

3.2. Microchip Microfabrication

Microchips were fabricated in four steps (Figure 9):

1. microfabrication of SU-8 masters of the micropillar and cover layers
2. casting of a poly(dimethyl siloxane) (PDMS) mold using the SU-8 master as a template
3. UV replica molding of the micropillar and cover layers in off-stoichiometric thiol-enes (OSTE) with the assistance of the PDMS molds
4. bonding of the OSTE micropillar and cover layers to obtain a sealed micropillar channel using lamination and UV-light.

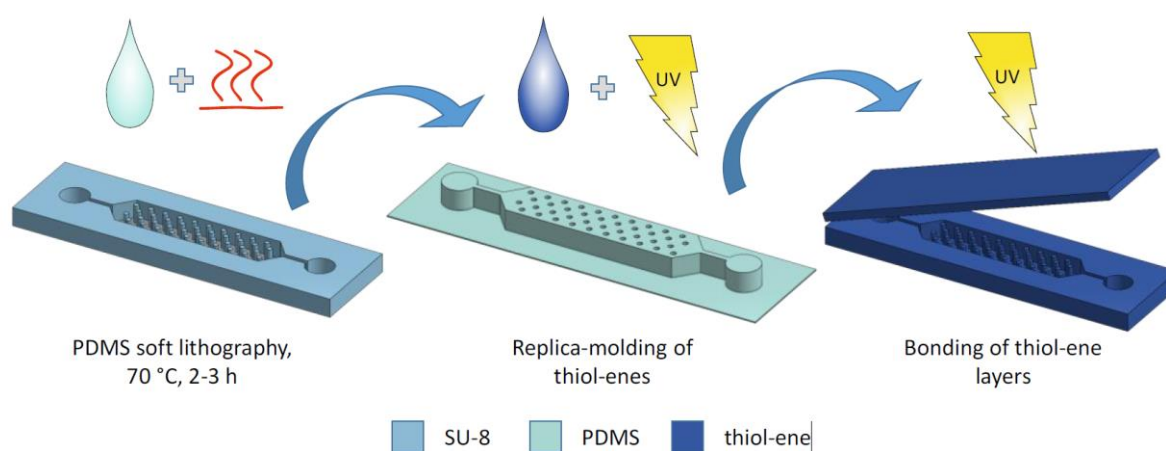


Figure 9. Microfabrication protocol (reproduced from Kiiski Iiro (2021) with permission of the author).

SU-8 masters were made by Dr Markus Haapala from the Faculty of Pharmacy, University of Helsinki following the UV photolithography protocol described in Tähkä *et.al.* (2019).

For the PDMS molds preparation, Sylgard 184 base elastomer and the curing agent were weighed and mixed in a 10 : 1 ratio (w/w) and intensively stirred. The mixture was degassed in vacuum for 30 minutes and cast onto the SU-8 master. Molds were put in the oven (80 °C overnight) in order to polymerize PDMS.

Triallyl and tetrathiol were mixed in off-stoichiometric ration with an excess of thiol groups. The mixture was poured out onto PDMS molds and after a few minutes of degassing in vacuum and manual removal of bubbles, the mixture was cured using UV (nominal power 225 mW/cm²) for 5 min.

Micropillar and cover layers were detached from PDMS molds, sealed manually and by additional UV-light curing.

Fabricated microchips contain one inlet where the feed solution containing substrates comes into the microchip and one outlet (Figure 10A) from which the solution containing metabolites is collected for further analysis. In the middle part of the microchips, a dense micropillar array is placed in a hexagonal lattice with approximately 14 400 micropillars, to increase the surface area available for enzyme immobilization (Figure 10B). Micropillar diameter is 50 μm with an interpillar (center-to-center) distance of 100 μm . The microchip's inner volume is ca. 25 μL .

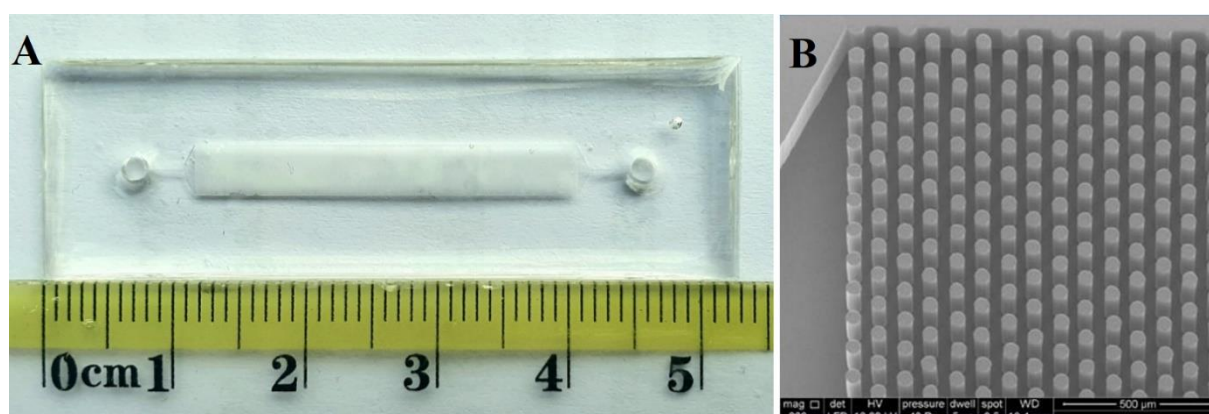


Figure 10. A) Appearance of the fabricated microchip – circles on the edge of the microchip are the inlet and the outlet, and the middle part is the micropillar array, where microsomes are immobilized in later steps, B) A light microscopy image of the micropillar array (reproduced from Kiiski Iiro, (2021) with permission of the author).

3.3. Microchip Functionalization and Immobilization of Human Intestinal Microsomes

Microchips were functionalized and enzymes were immobilized in four steps (Figure 11):

1. functionalization of the microchip with biotin, which bonds covalently with free thiol groups on the inside surface of the microchip
2. binding of streptavidin A (StrA) to biotin *via* a strong noncovalent bond
3. immobilization of biotinylated fusogenic liposomes (b-FL) to the microchip by noncovalent interactions of biotin from liposomes and streptavidin-coated microchip
4. fusion of HIM containing enzymes with previously immobilized b-FL.

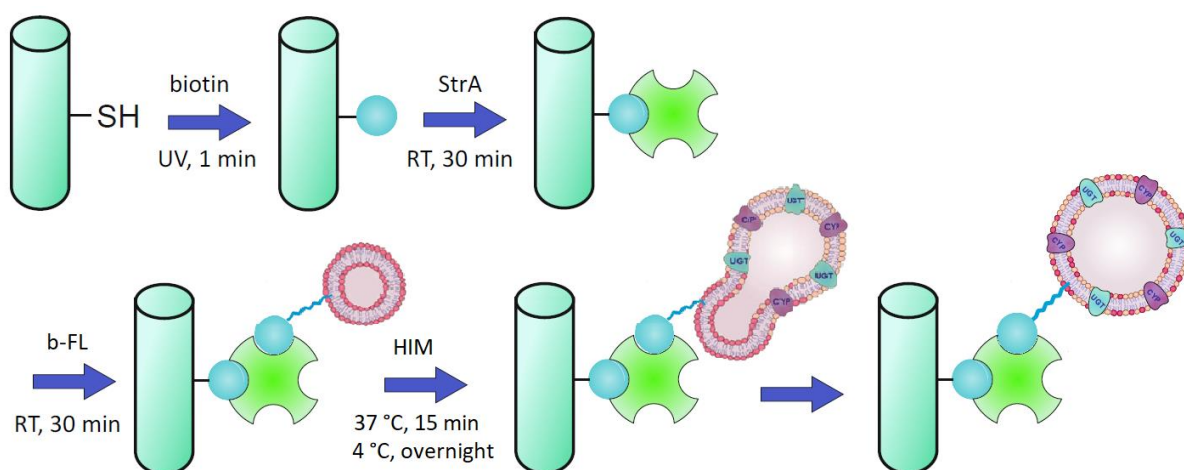


Figure 11. Functionalization and immobilization protocol. (adapted from Kiiski Iiro, (2021) with permission of the author).

To functionalize microchips with biotin, 28 μL of prepared biotin solution (biotin PEG4-alkyne 0,1 mM, lucirin 1% in MeOH, ethylene glycol) per microchip was pipetted in the microchips' inlet and pumped through the microchips followed by UV exposure (365 nm) for 1 min. Microchips were then washed with 5 mL of MeOH and 5 mL milli-Q water by pumping solutes through the microchips.

A prepared streptavidin solution (0.5 $\mu\text{g}/\text{mL}$ in 0.01 M PBS buffer, pH 7.4) was then pumped through the microchips (28 μL per microchip) and incubated for 30 min at room temperature to allow binding of streptavidin to biotin. Microchips were rinsed with 0.01 M PBS buffer, pH 7.4.

b-FL were prepared by the thin-film method, following previously established protocol by Kiiski *et al.*, (2019) as follows. Firstly, biotin-lipid mixture was prepared by mixing chloroform solutions of DOTAP (10 mg/mL), DOPE (10 mg/mL), biotin-DOPE (10 mg/mL), and lissamine rhodamine B-DOPE (1 mg/mL) lipids in a mass ratio 1 : 1 : 0.1 : 0.05. Chloroform was evaporated using nitrogen gas to form a thin lipid film, and residual solvents were removed using a vacuum desiccator for at least two hours. Next, lipids were dissolved in PBS buffer at room temperature and large multilamellar liposomes were formed with a total lipid concentration of 2 mg/mL. The suspension was then vortexed for one hour to ensure complete solvation. To form large unilamellar liposomes with fusogenic properties, a suspension of multilamellar liposomes was extruded through 0.1 μm porous polycarbonate membrane 51 times using Avanti syringe extruder.

Liposomes were then pumped through the chip following by a 30 min incubation at room temperature to allow immobilization of liposomes to streptavidin *via* a strong noncovalent interaction streptavidin-biotin.

HIM was diluted with 0.01 M PBS buffer, pH 7.4 to the final protein concentration of 1 mg/mL and were pumped through the chip followed by a 15 min incubation at 37 °C, and overnight at 4 °C to allow fusion of HIM and previously immobilized liposomes. Since the volume of the microchip's channel is ca. 25 μ L, the amount of protein used for preparation of one microreactor was ca. 25 μ g.

Microreactors were always rinsed with 5 mL of reaction buffer before use.

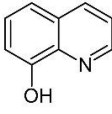
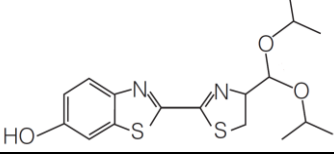
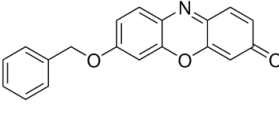
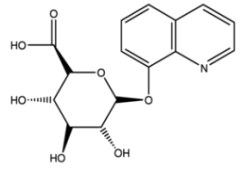
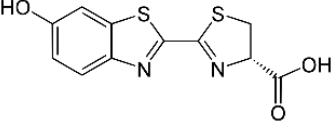
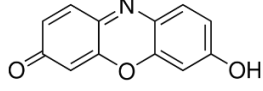
3.4. Size and ζ -Potential of Microsomes

For microsome size and ζ -potential measurement, microsome stocks were diluted with PBS to final concentration ready for measurement of 0.125 mg/mL. Instrument used for measurement was Zetasizer Nano ZS. Measurement consisted of 3 runs per sample with 11 measurements per run.

3.5. Model Reactions

For testing enzyme activity preservation after the immobilization, CYP3A4 and UGTs marker substrates were used. The following table (Table 5) contains information about model reactions and experimental setup.

Table 5. Information about model reactions.

Enzyme	UGT, various isoforms	CYP3A4	
Substrate name	8-hydroxyquinoline (8-HQ)	Luciferin-IPA	7-benzyloxyresorufin (BR)
Substrate structure			
Substrate concentration	50 μ M	3 μ M	2 μ M
Co-substrate	UDPGA	NADPH	NADPH
Co-substrate concentration	1 mM	1 mM	1 mM
Type of metabolic reaction	<i>O</i> -glucuronidation	<i>O</i> -dealkylation (dealcoxylation)	<i>O</i> -dealkylation (dealcoxylation)
Additional reagent*	50 μ g/mL Alamethicin (1% EtOH)	-	-
Metabolite	8-HQ-Glucuronide	<i>D</i> -Luciferin	Resorufin
Metabolite structure			
Contribution to organic solvent content	0.1% EtOH	0.3% DMSO	0.4% DMSO
Microsomes (protein concentration)	0.4 mg/mL	0.4 mg/mL	0.4 mg/mL
Reaction buffer	0.1 M Tris buffer, pH 7.4	0.1 M K-Phosphate buffer, pH 7.4	0.1 M K-Phosphate buffer, pH 7.4
Stopping reagent	4 M HClO ₄ , 10% v/v	Stopping reagent from the kit	2 M NaOH, 10% v/v
Detection	Fluorescence, ex: 245 nm, em: 475 nm	Luminescence	Fluorescence, ex: 572 nm, em: 590 nm

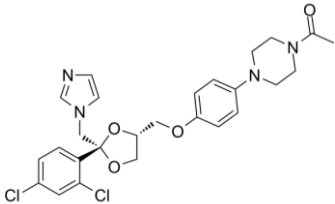
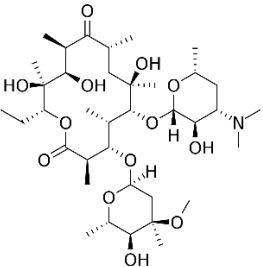
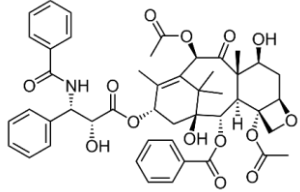
*only in static incubations

Even though fluorescence and luminescence are mostly not techniques of choice in drug research in pharmaceutical industry, but due to simplicity and substantially lower cost and higher throughput compared with liquid chromatographic analysis, these were the methods of choice for the development of the microreactor and acquiring proof of concept data. Consequently, in this work pre-fluorescent and pre-luminescent marker probes were used.

For a drug to reach UGTs' active site, it needs to first cross the microsomal/ER membrane. UGTs are showing the latency effect (Liu and Coughtrie, 2017) which reveals full UGT activity only after disruption of the microsomal membrane. This is why, in static incubations where UGT activity was measured, a peptide antibiotic alamethicin (which creates pores in the membrane) was added into the reaction. In contrast, it was shown that the addition of alamethicin to reactions, where microsomes are immobilized onto the microfluidic reactor, is not needed (Kiiski *et al.*, 2021).

In the later stage of experiments, CYP3A4 and CYP1B1 inhibitors were used to assess IMER as a platform for enzyme inhibition and drug-drug interaction research. Information about the used inhibitors is presented in the Table 6.

Table 6. Information about model inhibitors.

Inhibitor	Ketoconazole	Erythromycin	Paclitaxel
Inhibitor structure			
Inhibition towards	CYP3A4	CYP3A4	CYP1B1
Type of inhibition	Reversible, mixed competitive and non-competitive	Irreversible, mechanism-based, non-competitive	Reversible, competitive
IC ₅₀	0.04 μM	27.3 μM	31.6 μM
Elimination via	CYP3A4	CYP3A4	CYP3A4, CYP2C8
Inhibitor concentration	0-100 μM	0-100 μM	100 μM
Contribution to organic solvent content	0.4% DMSO	0.2% ACN	0.5% MeOH

*Data obtained in Table 6 is taken from (Kim *et al.*, 2017 Naritomi *et al.*, 2004;), (Fohner *et al.*, 2017; Coleman, 2010; Greenblatt *et al.*, 1998) and (Poeran, 2017; Spratlin and Sawyer, 2007) for ketoconazole, erythromycin and paclitaxel, respectively.

Wittingly high inhibitor concentrations were used to make sure that inhibition will happen, even though in high concentrations inhibitors become unselective.

Organic solvent content was always kept as low as possible, with the maximum content of 2% because it was shown that higher amounts of organic solvent have an inhibitory impact on CYP enzymes (Chauret *et al.*, 1998).

3.6. Implementation of Static Assays

The reaction volume was 100 μ L. Samples were prepared by addition of pre-calculated amounts of buffer, microsomes, and substrates. For inhibition experiments, the inhibitor was added before the reaction was initiated. All inhibitors used in this work, due to their low water solubility, were prediluted in an organic solvent. The same organic solvent content was maintained through all of the samples.

After a 5 min preincubation at 37 °C, the reactions were initiated by addition of NADPH or UDPGA. Incubation times were 10 or 15 min, all at temperature of 37 °C. Reactions were stopped by addition of a stopping reagent (10% v/v, or 50% for luciferin-IPA reaction), followed by sample centrifugation at 15000 rcf for 10 min. A volume of 100 μ L was transferred to Optiplate 96-well plate and a fluorescence or luminescence signal (Table 5) was measured. Additionally, a standard curve in buffer or in reaction matrix was prepared before the measurement.

3.7. Implementation of Flow-Through Assays

The feed solution containing the substrate and the co-substrate was prepared and put into a syringe connected by a tubing system to the IMER. The microchip was placed on the aluminium heating element that was placed on the hot plate with its own temperature regulation system (Figure 12 and Figure 13).

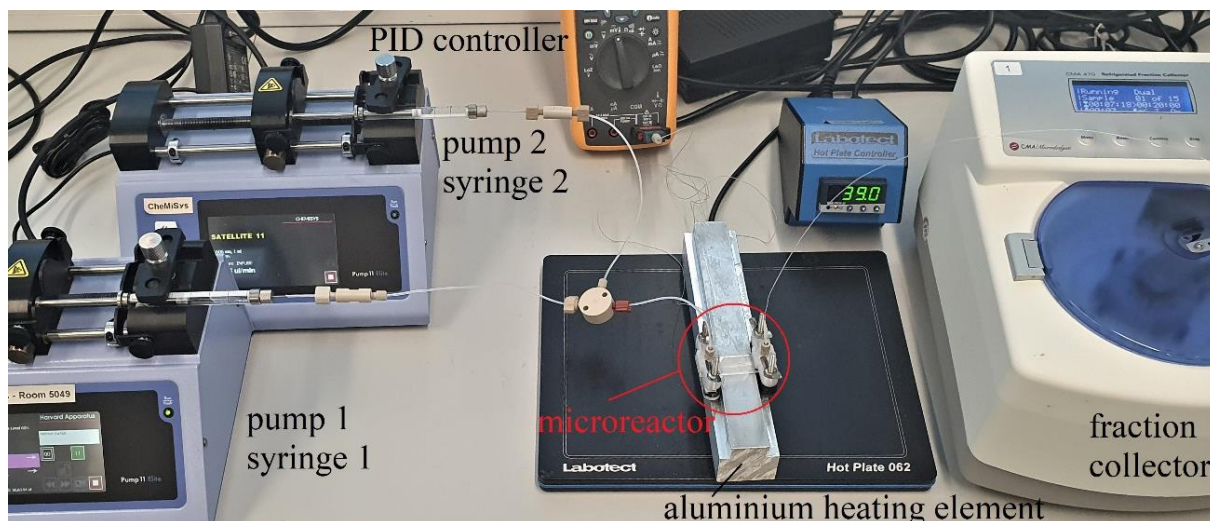


Figure 12. Components of IMER setup with two interconnected syringe pumps.

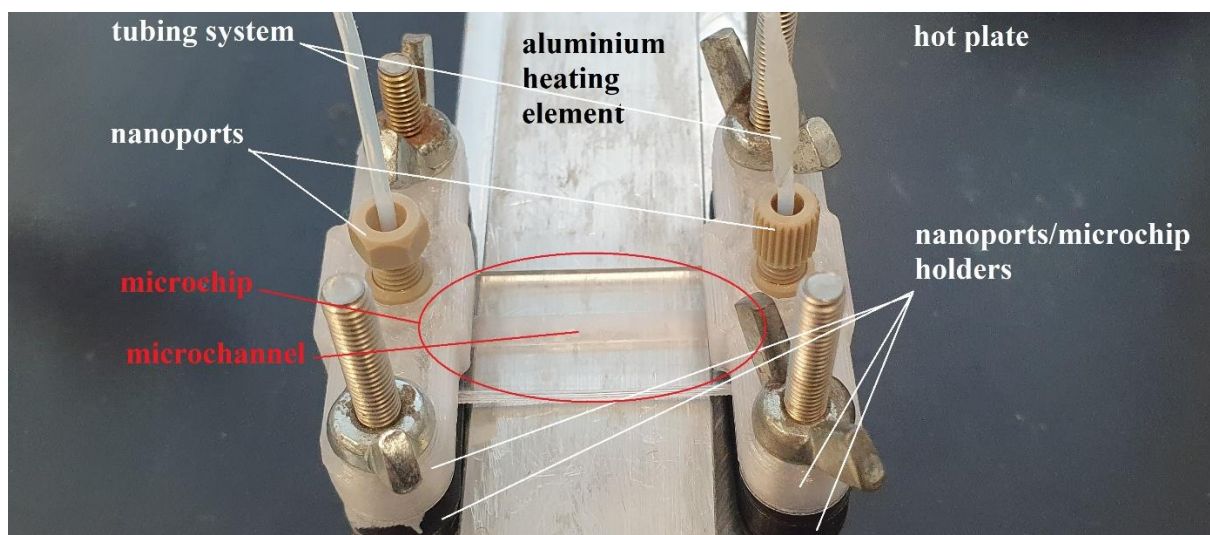


Figure 13. Components of IMER setup zoomed in.

The temperature of the hot plate was adjusted to 39 °C because in-house measurements showed that with this hot plate temperature, temperature inside the microreactor is 37 °C. The external syringe pump pumped the feed solution from the syringes through the microchip. First, a zero (dummy) fraction was collected containing mostly buffer which was inside the microreactor before the initiation of the experiment. A zero fraction was collected to assure filling of the microreactor with the feed solution and to assure stabilization of the system. Therefore, it was not included in the results. Next, after assuring there is no leakage of the feed solution from the microreactor, samples containing metabolites in the volume of 50 or 100 μL were collected

manually every 20 or 40 min of the run and kept covered on ice. Alternatively, collection was done using an automatic fraction collector and then incubated at 8 °C. Buffer was added to a specific fraction volume if some micro-leaking was present and the concentration of the metabolite was back-calculated accounting for the dilution factor. A substrate blank was taken from the syringe after the run. In experiments where stopping reagent was needed for reaction termination, after all fractions were collected, 10 µL of a stopping reagent was added to each sample to allow for a more precise comparison to static experiments. A sample volume of 100 µL was transferred to Optiplate 96 well plate and analysed by plate reader. Additionally, a metabolite standard curve in buffer or reaction matrix for CYP or UGT reactions, respectively, was prepared before every measurement. Volume of the standard was the same as the volume of the samples.

For the flow-through inhibition experiments, a setup with two interconnected pumps was used (Figure 12). Pump 1 was the main pump and its syringe contained only the substrate and the co-substrate in the reaction buffer. Pump 2 pumped the feed solution from syringe 2 containing the substrate and the co-substrate in the reaction buffer in the same concentration as in syringe 1 + inhibitor in its maximal concentration used in the experiment. By controlling the ratio of feed solutions coming from two different syringes, the final solution entering the microchip contained inhibitor in concentration gradient. This was achieved by programming the pumps to pump continuously together, each by its own flow rate, always with the same total flow rate (flow rate in the pump 1 + flow rate in the pump 2). After every flow rate change, one zero (dummy) fraction was collected. A setup example of the experiments with two pumps is shown in Table 7.

Table 7. Setup example of the experiment with two pumps

run time	volume of the fraction (μL)	sample name	pump 1 (%)	flow rate pump 1 ($\mu\text{L}/\text{min}$)	pump 2 (%)	flow rate pump 2 ($\mu\text{L}/\text{min}$)	Ketoconazole conc. (μM)	Other reagents conc.
20 min	100	dummy1	100	5.0	0	0.0	0	BR: 2 μM
40 min	100	1						
1 h	100	2						
1 h and 20 min	100	dummy2	50	2.5	50	2.5	50	NADPH: 1 mM
1 h and 40 min	100	3						
2 h	100	4						
2 h and 20 min	100	dummy3	0	0.0	100	5.0	100	Paclitaxel: 100 μM
2 h and 40 min	100	5						
3 h	100	6						
3 h and 20 min	100	dummy4	100	5.0	0	0.0	0	8-HQ: 50 μM UDPGA: 1 mM
3 h and 40 min	100	7						
4 h	100	8						
4 h and 20 min	100	9						
4 h and 40 min	100	10						

3.8. Quantification of Enzymes Immobilized

For calculation of the amount of enzyme immobilized to the microchip, the first fractions collected were analysed and the amount of protein in these fractions was calculated. The flow rate in this experiment was 20 $\mu\text{L}/\text{min}$ and fractions of 50 μL were collected. Pierce™ BCA Protein Assay Kit, based on the biuret reaction, was used for quantification. Colorimetric measurement of protein amount was done according to the protocol provided by supplier. Obtained protein amount was used for immobilization yield calculation.

4. RESULTS AND DISCUSSION

4.1. Comparison of HIM and HLM

The aim of this work was to develop a first in its kind microfluidic enzyme microreactor with immobilized human intestinal microsomes. Prior to development of IMERs for intestinal drug metabolism research, HIM was characterised and compared to HLM in the terms of enzyme activity, microsome size, and microsome ζ -potential.

4.1.1. Enzyme Activity

Static incubation experiments where HIM enzyme activity was measured, served as a reference point for future IMER experiments. Furthermore, a comparison of enzyme activity in static conditions between HIM and HLM is important because it could indicate possible detection problems in IMER setup with HIM, which were not present with HLM. This is due to previously reported results indicating that enzyme activity in HIM is generally lower than in HLM (Dressman and Thelen, 2009) and the fact that amount of protein used for enzyme immobilization is lower than amount of protein used in static incubations.

CYP3A4 is reported to be most abundant enzyme in HIM and most significant for the total intestinal metabolism (Gundert-Remy *et al.*, 2014; Paine *et al.*, 2006;). Hence, in this work it was chosen to observe only CYP3A4 activity. For this purpose, a commercially available kit with a substrate specific for CYP3A4 was used. At this stage, only the relative difference in activity between HIM and HLM was of importance, so activity was represented as luminescence signals coming from luciferin, which is the metabolite produced.

Results showed that CYP3A4 activity in HIM is lower than in HLM (Figure 14).

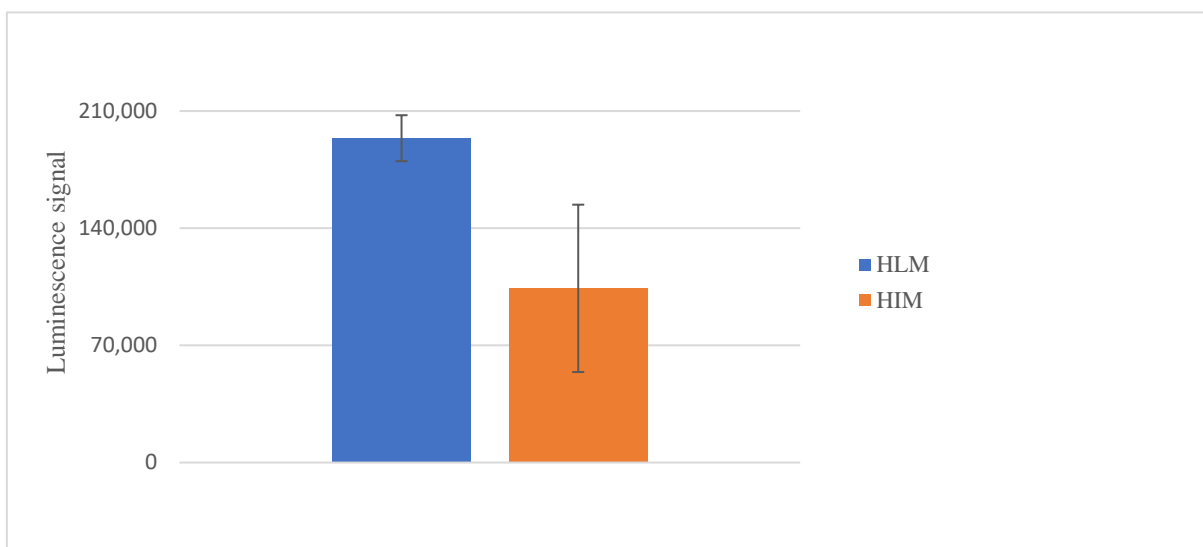


Figure 14. Comparison of CYP3A4 activity in HLM and HIM ($N = 4$, 10 min static incubation, 37 °C, microsome conc.: 0.4 mg/mL, substrate conc.: 3.0 μ M luciferin-IPA). N corresponds to the number of replicates.

The activity of UGT enzymes was also tested (Figure 15). For the substrate, 8-hydroxyquinoline (8-HQ), standard chemical probe for studying UGT enzymes was used.

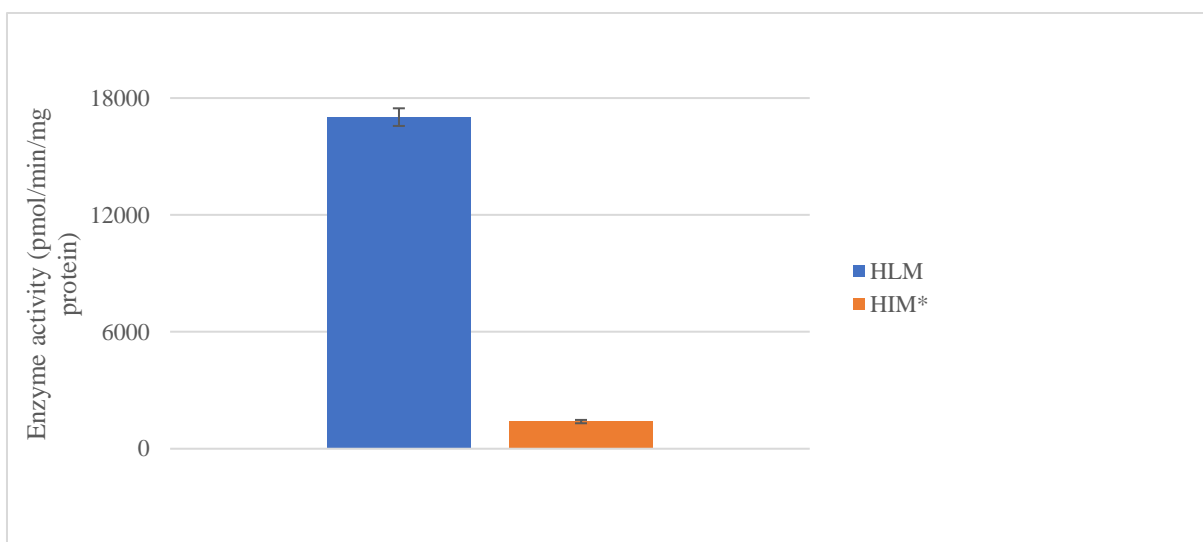


Figure 15. Comparison of UGT activity in HLM and HIM ($N = 4$, 10 min static incubation, 37 °C, microsome conc.: 0.4 mg/mL, substrate conc.: 50.0 μ M 8-HQ), *LOT number of HIM used in this experiment was different than LOT number of HIM used in other experiments. N corresponds to the number of replicates.

From the results it was visible that UGT activity in HIM was also lower than in HLM.

Both HLM and HIM are defined by total protein content (mg/mL) and in all experiments the amount of protein used (coming from HLM or HIM) was 40 μ g. Since this value represents the total protein content in microsomes, and not just metabolic enzymes content and because liver is the main organ responsible for metabolism, it was expected that the enzyme activity in HIM will be lower than in HLM. This also corresponds to results reported in the literature (Dressman and Thelen, 2009).

4.1.2. Size and ζ -Potential

Microsome size and ζ -potential are physical properties of microsomes and are important for their fusion with liposomes, which is a step in microsome immobilization. Fusion of liposomes with microsomes is based on opposite net charges (positive ζ -potential values for liposomes and negative ζ -potential values for microsomes). These parameters were measured in order to check if previously established protocols for HLM immobilization (Kiiski *et al.*, 2019) could be adapted to HIM immobilization. Results are shown in Table 8.

Table 8. Comparison of size and ζ -potential of HLM and HIM (N=3). N corresponds to the number of replicates.

Microsome type	Size (nm)	ζ -potential (mV)
HLM	249.7 \pm 3.0	-32.7 \pm 0.3
HIM	198.6 \pm 1.8	-33.9 \pm 1.3

Both HLM and HIM have similar size and negative ζ -potential values which enable adaptation of the previously established HLM immobilization protocol for HIM immobilization (Kiiski *et al.*, 2019).

4.2. Optimization of the Immobilization Method

The immobilization protocol was adapted from Kiiski *et al.* (2019) where human liver microsomes were used. Due to a higher cost of HIM, the protocol was modified so HIM usage would be 5-fold lower. The new, optimized protocol is described in detail in section 3.3.. The differences between the protocols are shown in Table 9, and the comparison of obtained enzyme activity in IMERs prepared by two different immobilization protocols are shown in Figure 16. In this experiment, UGT activity was measured.

Table 9. Procedural differences between old (based on Kiiski et al. (2019)) and new (optimized) immobilization method. HIM concentration is defined by supplier as a total protein content (mg/mL) from which the amount of protein used was calculated.

	Amount of protein used per one microchip (μg)	Immobilization protocol
Method based on Kiiski et al. (2019.)	125	1. fusion of HIM and biotinylated liposomes outside of the microchip to form b-HIM (final protein concentration is 5 mg/mL) 2. immobilization of b-HIM by applying 25 μL of b-HIM into the microchip
Optimized method	25	1. immobilization of biotinylated liposomes by applying 25 μL of biotinylated liposomes into the microchip 2. fusion of HIM with immobilized liposomes by applying 25 μL of 1 mg/mL HIM into the microchip

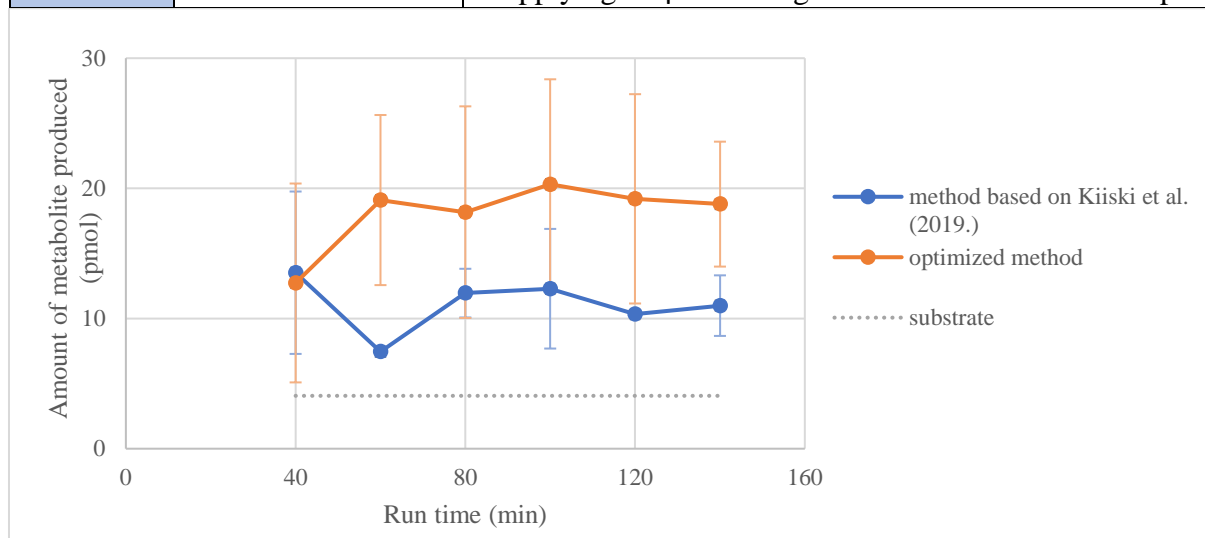


Figure 16. Comparison of obtained HIM enzyme activity in IMERs prepared by the method based on Kiiski et al. (2019.) and optimized immobilization method ($N = 3$, $37\text{ }^{\circ}\text{C}$, flow rate: $2.5\text{ }\mu\text{L}/\text{min}$, substrate: $50\text{ }\mu\text{M}$ 8-HQ. N corresponds to the number of replicates.

To begin with, a difference in values between collected samples and the substrate blank immediately shows that UGT activity was preserved after immobilization. More importantly, results showed that not only the new, optimized method was better because of the 5-fold higher microsomes savings, but the new protocol had a higher immobilization efficiency. However, new, optimized protocol had seemingly a bit higher chip-to-chip variation (error bars). Because of abovementioned, the optimized protocol was used in all assays that would follow. A more detailed difference analysis between the two methods and the reason behind a higher immobilization efficiency with the optimized method are beyond the scope of this thesis.

4.3. Finding Suitable Marker Substrates

To characterize established IMERs, marker reactions used in static incubations need to also be suitable for IMER setup. Besides the already presented UGT activity preservation in IMER setup (Figure 16), CYP3A4 activity was tested too.

The same CYP3A4 specific kit used in static incubations was tested in IMER setup. Enzymes were immobilized by new, optimized immobilization protocol (Figure 17).

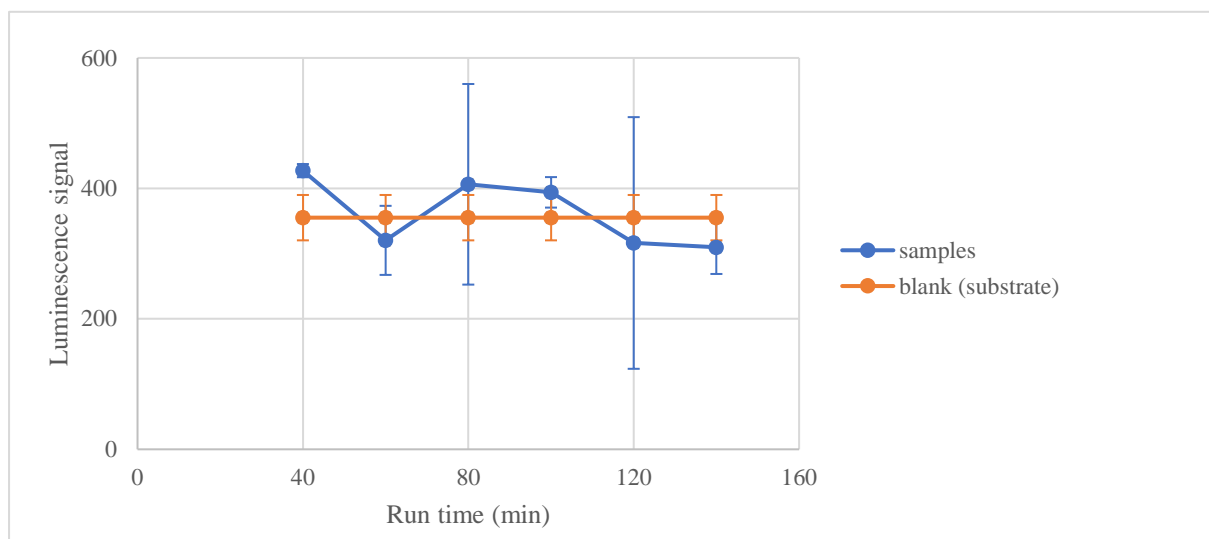


Figure 17. Suitability of luciferin-IPA as a CYP3A4 marker substrate in IMER setup, expressed as an average signal coming from the metabolite measured in fractions collected every 20 min of the run ($N = 3$, $37\text{ }^{\circ}\text{C}$, flow rate: $2.5\text{ }\mu\text{L}/\text{min}$, substrate: $3.0\text{ }\mu\text{M}$ luciferin-IPA).

Signals measured in fractions collected from the microchip did not differ from the substrate (blank) signal, which in contrast to other collected samples, did not pass through the microchip with immobilized enzymes. Signals were not affected by storing conditions because both the feed and the eluted fractions were treated similarly and stored at room temp for equally long time. Some of the reasons behind not finding any metabolite in the collected fractions could be: i) fairly low CYP3A4 activity in the HIM, ii) the loss of CYP3A4 enzyme activity during the immobilization process, iii) non-specific binding of the substrate or the metabolite to the components of the microchip which includes thiol-enes, biotin, streptavidin, and lipid membranes, iiiii) degradation of metabolite before detection. Even though presence of CYP3A4 activity in HIM was shown in static assays, it is possible that signals obtained in IMER setup are below limit of detection (LOD) since there is fewer active enzymes immobilized on IMER than it was present in static incubations.

4.3.1. Screening of New Pre-fluorescent CYP3A4 Probes

Due to unsuitableness of luciferin-IPA for IMER experiments, new CYP3A4 substrate was needed. Chosen probes for primary screening of CYP3A4 activity in HIMs were 7-benzyloxy-4-trifluoromethylcoumarin (BFC), dibenzylfluorescein (DBF), 7-benzyloxyquinoline (HQ), and 7-benzyloxyresorufin (BR), for which extensive metabolism by CYP3A4 was reported in the literature (Stresser *et al.*, 2002). These probes were not selective for CYP3A4, however, assuming that CYP3A4 is the most abundant enzyme in HIM, it was assumed that their transformation rate will well reflect CYP3A4 activity. Based on internally-made primary screening results in static incubations with HIM (not presented in the thesis), DBF and BR were chosen for testing in the IMER setup.

The first pre-fluorescent substrate tested in IMER setup was DBF, but similarly to experiment with luciferin-IPA, no significant activity was observed with DBF in HIM-IMERs. Possible explanations for this are similar to the case with luciferin-IPA. Deep understanding of this effect is beyond the scope of this thesis, but it should be studied in the future works.

The second pre-fluorescent substrate that showed potential in the static experiment was BR, and it was tested in the IMER setup (Figure 18). In this experiment, the difference in obtained signals between the substrate and samples collected is considerable, which indicates that immobilized HIM on microreactor surface exhibit CYP3A enzyme activity.

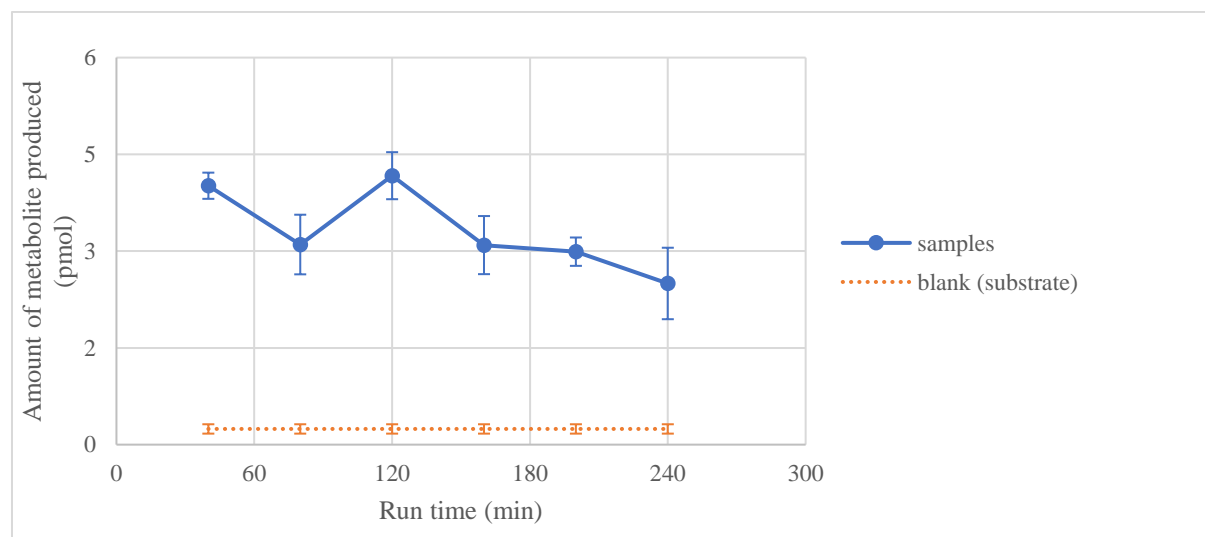


Figure 18. Suitability of BR as a CYP3A marker reaction in IMER setup, expressed as an average signal coming from the metabolite measured in fractions collected every 40 min of the run ($N = 3$, $37\text{ }^{\circ}\text{C}$, flow rate: $2.5\text{ }\mu\text{L}/\text{min}$, substrate: $2.0\text{ }\mu\text{M}$ BR). N corresponds to the number of replicates.

4.4. IMER Characterisation

After finding an appropriate CYP3A4 pre-fluorescent substrate, it was possible to characterise IMER in the terms of enzyme immobilization yield, enzyme activity, and enzyme stability.

4.4.1. Enzyme Immobilization Yield

Immobilization yield was determined by colorimetric measurement of the amounts of enzymes in the first IMER washing fractions 24 hours after immobilization and compared to the amount of enzymes used for immobilization. It was shown that unbound microsomes eluted from the microchip in the first 200 μL of washing solution, where most of the unbound microsomes were washed with the first 50 μL .

Table 10. Enzyme immobilization yield (N=4). N corresponds to the number of replicates.

amount of protein pumped into one microchip:	25 μg
Average % of HIM immobilized	85.60 %
Standard deviation	7.04 %

Obtained results (Table 10) indicate that immobilization was accomplished successfully, with an average of 85.6% of microsomes being immobilized (as per total protein amount). However, chip-to-chip variation was high, even though they were all fabricated under the same conditions. Possible explanation could be in different area available for immobilization. If during fabrication some bubbles of air were kept between micropillars, these areas would not be available for immobilization and consequently immobilization yield would be lower. However, this was tried to be avoided by pipetting out bubbles.

It is important not to substitute immobilization yield with activity recovery since not all microsomes immobilized necessarily kept their activity. Another point is that IMERs with higher immobilization yields have not produced more metabolites in later experiments (activity recovery). This could indicate that the immobilization efficiency between IMERs also differs significantly. Storing conditions can affect enzyme activity - exposure to air can cause drying and, thereby, be detrimental to enzyme activity, however the risk of that was minimized by keeping the microchip's inlet and outlet sealed with parafilm when not in use.

Already from these results, reproducibility is seen as one of IMERs' drawbacks in this work. With a large standard deviation already within the immobilization step, and observed activity

not being in the correlation achieved immobilization yield, it is hard to expect uniform results in the rest of the experiments.

4.4.2. Enzyme Activity

Evaluation of enzyme activity (activity recovery) is not straightforward because of high chip-to-chip variation and due to the major differences between IMER setup and conventional static assays.

First, in a static incubation setup, 40 μg of protein (from HIM) was used per sample and for each IMER only 25 μg of protein was applied into the chip to immobilize it. Another difference is the terms in which reaction time is described. Conventional incubation time does not exist in flow-through conditions, but instead, it is described as residence time – the time which one molecule spends in the microreactor while traveling from one side of the microreactor to another. Residence time is inversely proportional to flow rate and the microreactor volume. Since the microreactor volume is around 25 μL , the flow rate of 2.5 $\mu\text{L}/\text{min}$ and 5 $\mu\text{L}/\text{min}$ corresponds to 10 min and 5 min incubation time in static incubations, respectively.

Even though IMER enzyme activity could be calculated (pmol of metabolite produced *per* residence time in min *per* mg of protein immobilized), and activity recovery derived from it, due to the high chip-to-chip variation in immobilization yield and immobilization efficiency, calculated result would not be confident. Because of the same reason, all IMER results are shown as signals, normalized signals, or amounts of metabolite produced and not as enzyme activity.

4.4.3. Stability of the Enzyme Activity under Flow-Through Conditions

One of the greatest IMER advantages is the possibility of reusing it. In particular, more than one experiment with different substrate solutions can be performed on the same IMER with the washing step in between.

To test the stability of the prepared IMER, an amount of metabolite produced over more than eight hours run was observed (Figure 19).

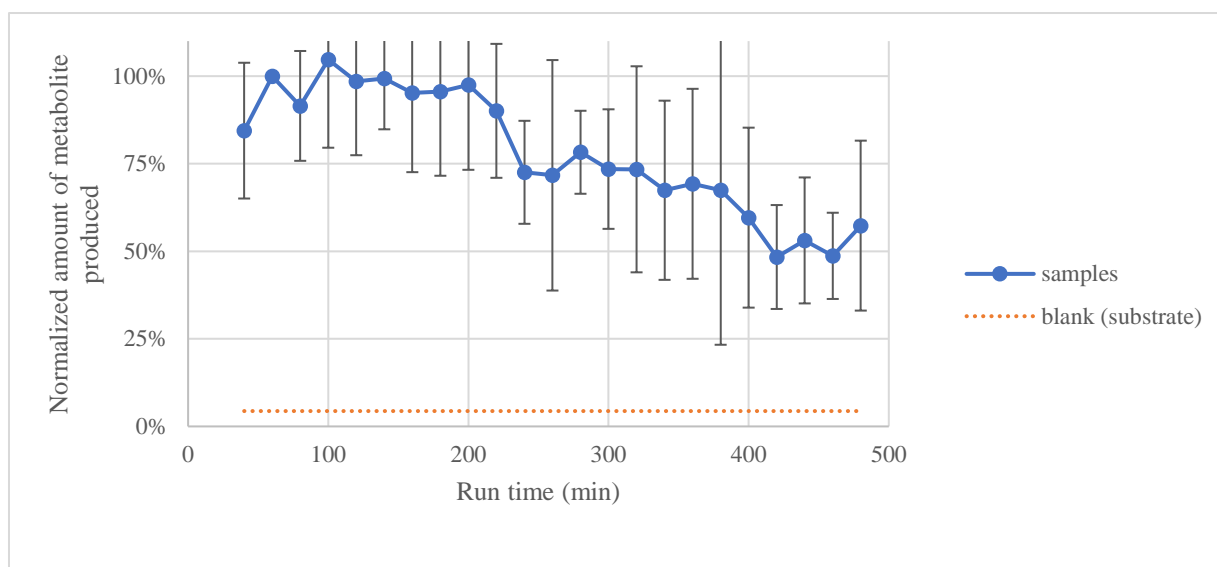


Figure 19. Stability of enzyme activity under the flow-through conditions, expressed as an average normalized amount of metabolite produced in different time points of the run. Amounts of metabolite produced were normalized by division by the amount of metabolite produced in the second fraction collected ($N = 4$, $37\text{ }^{\circ}\text{C}$, flow rate: $5.0\text{ }\mu\text{L}/\text{min}$, substrate: $2.0\text{ }\mu\text{M BR}$). N corresponds to the number of replicates.

Results showed that the developed IMER is stable during the first three hours of run time, after which enzyme activity decreases. A decrease in enzyme activity seems to be an intrinsic property of microsomes since this effect can be observed in static incubations as well. Even though enzyme activity eventually decreases with time, IMER could still be used. More precisely, using IMER as a platform for production of metabolites of interest could be convenient. For the kinetic experiments lasting longer than a few hours obtained values should be corrected by the % of loss of enzyme activity over time (Schejbal *et al.*, 2016).

4.5. IMER Setup as a Concept for Assessment of Drug-Drug Interactions

An important application of the IMER setup is using it for drug-drug interaction assays. With the use of continuous flow, where the composition of the feed solution can be altered to contain different concentrations of substrates/inhibitors in different time points, type of inhibition and inhibition parameters can be determined in only one experiment.

4.5.1. Comparison of Inhibition of CYP3A4 Activity by Ketoconazole in HIM and HLM

Before performing inhibition assays in IMER setup, inhibition of BR transformation in HIM and HLM by ketoconazole was first confirmed with a conventional, static setup. A series of samples with different ketoconazole concentrations ranging from 0 to 100 μM was prepared and the activity of BR dealcoxylation was measured. Experiment results are shown in Figure 20.

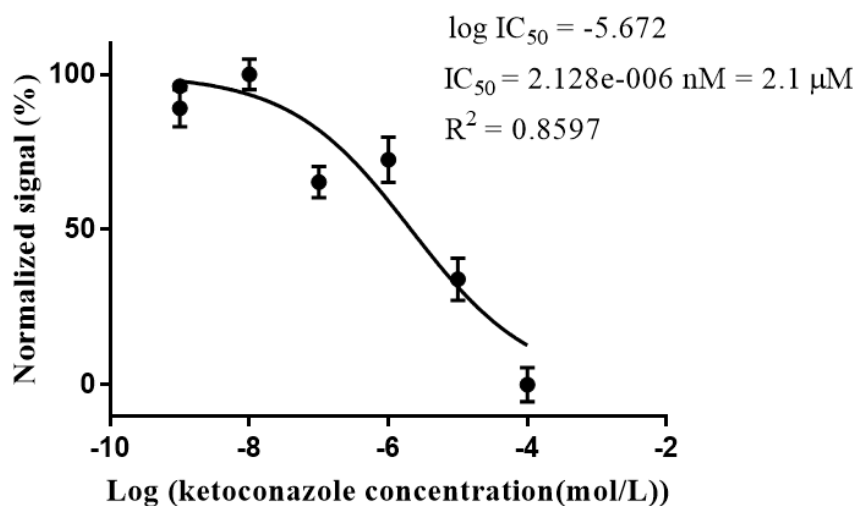


Figure 20. Inhibition of CYP3A4 activity in HLM by ketoconazole in a concentration range of 0-100 μM , using BR as a marker substrate ($N = 4$, 15 min static incubation, 37 $^{\circ}\text{C}$, microsome concentration: 0.4 mg/mL, substrate concentration.: 2.0 μM BR). N corresponds to the number of replicates.

Data obtained from HLM inhibition experiments allowed calculation of ketoconazole IC_{50} . The obtained results differ from the results in the literature (with BR as a substrate): 2.1 μM and 0.04 μM (Naritomi *et al.*, 2004), respectively. Significant differences between the calculated ketoconazole inhibition parameters, even when using the same substrate were already reported, but not completely explained (Greenblatt *et al.*, 2010).

The same experiment performed with HIM, instead of HLM did not show any inhibition (Figure 21). Interestingly, the results showed that BR transformation was inhibited by a CYP3A4 inhibitor – ketoconazole, in HLM, but not in HIM. Since ketoconazole is a well-known CYP3A4 inhibitor, these results suggest that BR is effectively metabolized in HIM by some other enzymes.

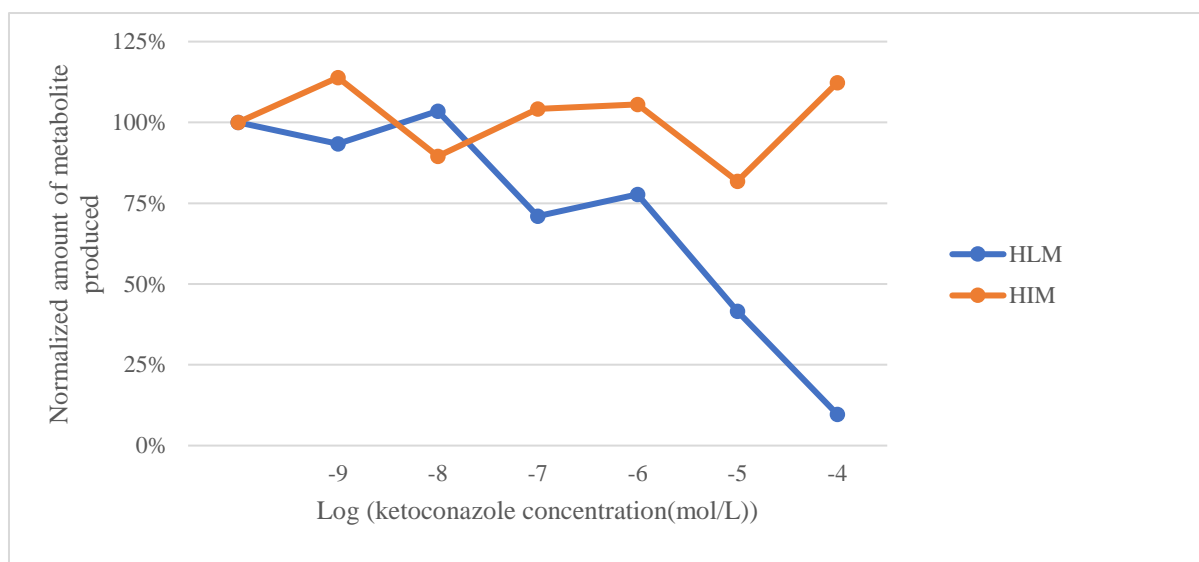


Figure 21. Comparison of CYP3A4 activity inhibition in HLM and HIM by ketoconazole in concentration. range of 0-100 μ M, using BR as a marker substrate ($N = 2$, 15 min static incubation, 37 $^{\circ}$ C, microsomes concentration: 0.4 mg/mL, substrate concentration: 2.0 μ M BR). N corresponds to the number of replicates.

BR is a CYP substrate and could be transformed to resorufin by a few CYP isoforms, including CYP1B1, CYP1A1, CYP3A4, CYP3A7, CYP2B6, CYP3A5, CYP26, CYP1A2, with CYP1B1 having almost 20-fold higher turnover rate (pmol of product *per min per* pmol of recombinant enzyme) than CYP3A4 (Stresser *et al.*, 2002). Even though CYP1B1 has the highest turnover rate, due to its low expression in HLM, it is not the most important CYP isoform for BR transformation in hepatic tissues. Therefore, it is possible to see inhibition of BR metabolism by inhibition of CYP3A4.

Since there is no strong evidence of CYP1B1 expression in HIM (Dressman and Thelen, 2009; Paine *et al.*, 2006), and in addition there is no information about CYP1A activities in HIM from the supplier (section 9.1.1., Table 11), before performing experiments, it was assumed that CYP3A4 is the isoform the most responsible for BR metabolism in HIM. However, HIM is prepared from intestine of five different human donors and there may be large interindividual variation in enzyme expression. No inhibition of BR metabolism in HIM by a CYP3A4 inhibitor ketoconazole indicates that there is another CYP isoform mostly responsible for BR transformation in HIM, most likely CYP1B1 due to its high turnover rate.

4.5.2. Comparison of BR Transformation in HIM and HLM

To confirm if BR is mostly metabolized by a CYP isoform different than CYP3A4, first, both HIM and HLM were incubated with BR and NADPH under the same conditions and the signal coming from the metabolite, resorufin, was measured (Figure 22).

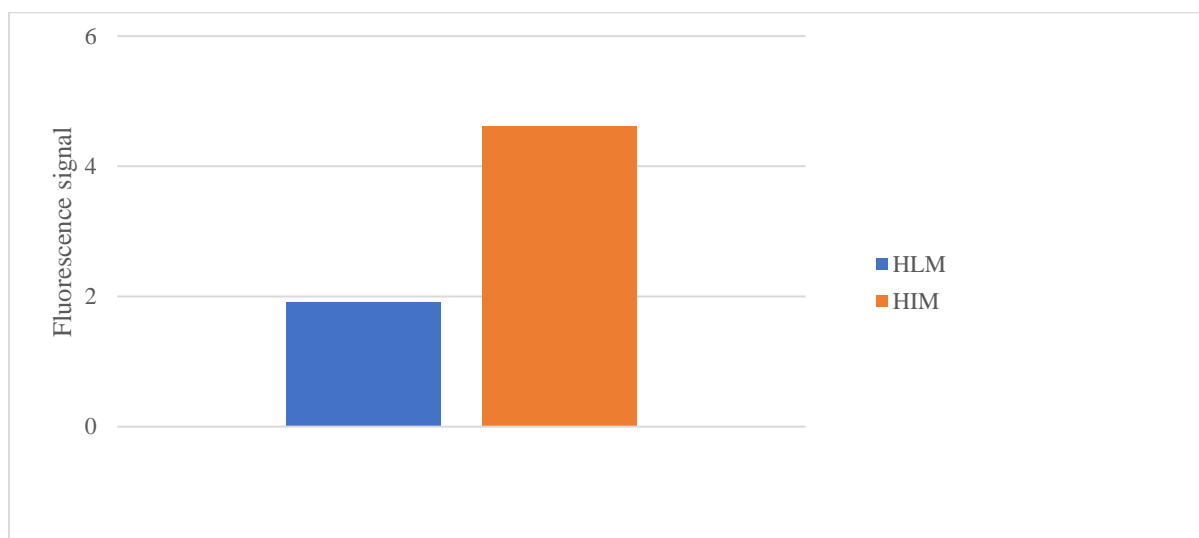


Figure 22. Comparison of BR transformation in HLM and HIM ($N = 2$, 15 min static incubation, 37 °C, microsomes concentration: 0.4 mg/mL, substrate concentration: 2.0 μ M BR). N corresponds to the number of replicates.

Results showed that the amount of metabolite produced in HIM is higher than in HLM, which is in contrast with the results obtained in static incubation experiment with luciferin-IPA as a substrate specific for CYP3A4 (Figure 14), and in contrast with the literature, where a higher HLM activity in comparison to HIM is reported (Dressman and Thelen, 2009). This indicates that BR in HIM is indeed transformed to resorufin by some other CYP isoform, which has a higher turnover rate than CYP3A4 because CYP3A4 is still the most abundant CYP isoform in HIM.

4.5.3. Inhibition of BR Transformation by CYP1B1 Inhibitors

After the theory of BR being metabolised by a CYP isoform different than CYP3A4 was shown to be plausible, discovering its identity was the next goal. CYP1B1 is a CYP isoform with the highest BR turnover rate and, therefore, was chosen for testing, even though its expression in HIM was not confirmed or reported in the literature.

To test this theory, BR metabolism was attempted to be inhibited by a CYP1B1 inhibitor. Paclitaxel is a competitive CYP1B1 inhibitor with K_i of 31.6 μM (Rochat *et al.*, 2001), and it was chosen for the following experiments. Paclitaxel is metabolized by CYP3A4 and CYP2C8 (Spratlin and Sawyer, 2007), so in order for it to be available for inhibition of CYP1B1, its metabolism also needs to be inhibited. According to the literature, CYP2C8 should not be too abundant in HIM (Paine *et al.*, 2006), and therefore there was no need for CYP2C8 inhibition. As a result, paclitaxel metabolism would be inhibited by ketoconazole and erythromycin, both CYP3A4 inhibitors.

Concentrations in this experiment were exaggerated to assure inhibition. At the same time, choosing high concentration of paclitaxel led to formation of precipitate in the test tube due to its poor solubility. Results of the experiment are shown in Figure 23.

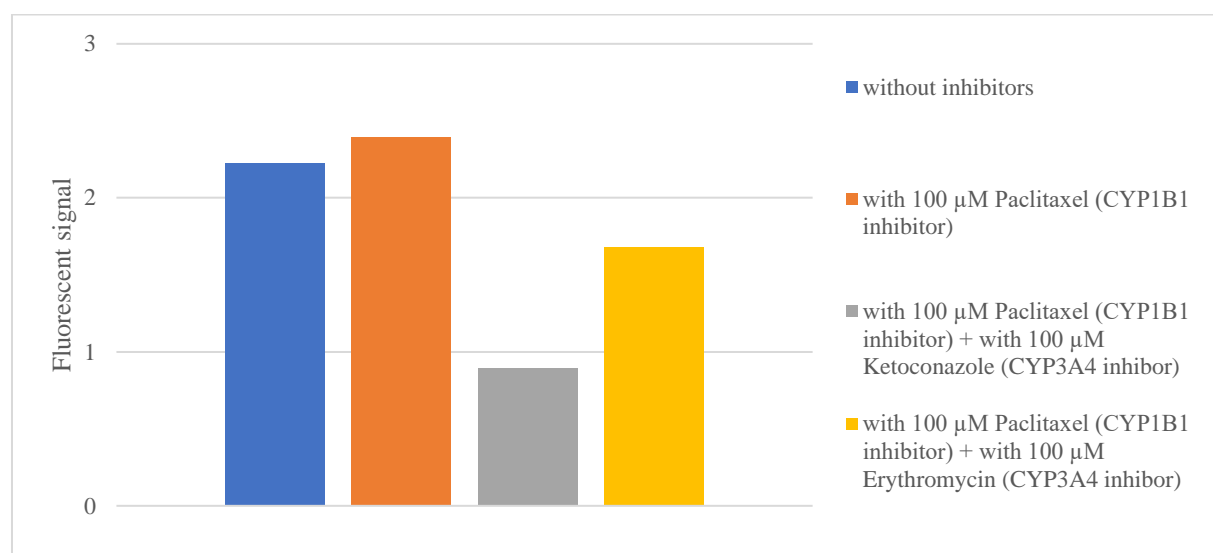


Figure 23. Inhibition of BR transformation by the combination of CYP1B1 (paclitaxel) and CYP3A4 (ketoconazole) inhibitors, expressed as an amount of metabolite produced ($N = 2$, 15 min static incubation, 37 $^{\circ}\text{C}$, microsome concentration: 0.4 mg/mL, substrate concentration: 2.0 μM BR). N corresponds to the number of replicates.

Due to a shortage of microsomes, this experiment was performed only in duplicates, which is not enough for a statistical data processing (t -test), so further confirming experiments are needed. However, it could be concluded that BR metabolism in HIM is inhibited by a CYP1B1 inhibitor – paclitaxel, and that this inhibition is possible only if the paclitaxel availability is assured by inhibition of its own metabolism by a CYP3A4 inhibitor, ketoconazole and less by erythromycin. At high concentrations ketoconazole also inhibits other CYP enzymes, while erythromycin on the other hand should be rather specific CYP3A4 inhibitor even at high

concentrations. Therefore, ketoconazole causes broader inhibition and thereby inhibits paclitaxel metabolism more extensively and consequently results in more prominent CYP1B1 inhibition by paclitaxel.

The inhibition of BR dealcoxylation in HIM, obtained via inhibition of paclitaxel metabolism to reveal its inhibitory potential toward CYP1B1 (the enzyme presumable responsible of the metabolism of BR in HIMs) was reproduced on the IMERs.

The setup for the experiment is described in detail in section 3.7. and Table 7. The feed solution containing different concentrations of ketoconazole, ranging from 0 to 100 μM , passed through the microchip and the amount of resorufin produced was measured (Figure 24). Paclitaxel precipitate was again formed in the syringe, but since the flow rate in the experiment was low, it did not cause clotting.

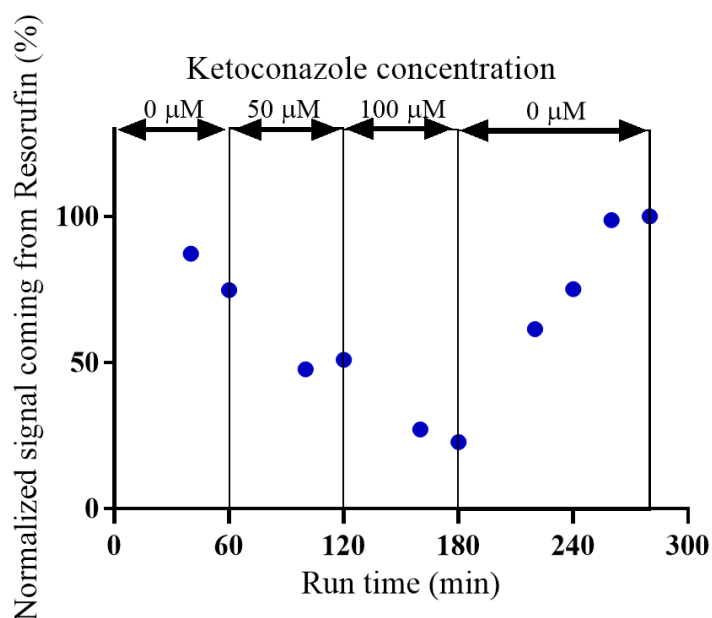


Figure 24. Effect of the increase and decrease of ketoconazole concentration on BR transformation when incubated with paclitaxel, expressed as an amount of metabolite produced ($N = 2$, $37\text{ }^{\circ}\text{C}$, flow rate: $5.0\ \mu\text{L}/\text{min}$, substrate: $2.0\ \mu\text{M}$ BR, $50.0\ \mu\text{M}$ 8-HQ). Data points on the vertical lines belong to the step prior to the line. N corresponds to the number of replicates.

Results showed that with an increase in ketoconazole concentration (from 0 to 100 μM during the first three steps), the BR dealcoxylation activity decreases (due to paclitaxel-induced inhibition), and after removing ketoconazole from the feed solution (after 180 min, fourth step),

the system recovered quickly, *i.e.*, the BR dealcoxylation activity rises immediately, which indicates that ketoconazole is a reversible inhibitor.

The feed solution contained not only substrates for transformations mediated by CYP, but also substrates for transformations mediated by UGT enzymes. Ketoconazole should not affect transformation of 8-HQ to 8-HQ-Glu because it does not inhibit UGTs. This was tested and the results are shown in Figure 25.

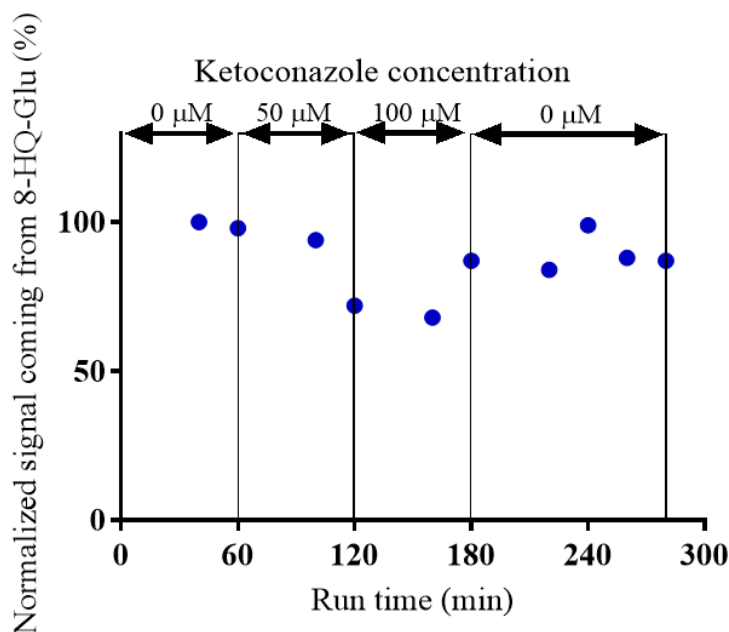


Figure 25. Effect of the increase and decrease of ketoconazole concentration on 8-HQ transformation when incubated with paclitaxel, expressed as an amount of metabolite produced ($N = 2$, $37\text{ }^{\circ}\text{C}$, flow rate: $5.0\text{ }\mu\text{L}/\text{min}$, substrate: $2.0\text{ }\mu\text{M}$ BR, $50.0\text{ }\mu\text{M}$ 8-HQ). Data points on the vertical lines belong to the step prior to the line. N corresponds to the number of replicates.

From the results, it is visible that at one out of two data points where ketoconazole concentration is $50\text{ }\mu\text{M}$, and one out of two data points where ketoconazole concentration is $100\text{ }\mu\text{M}$, the signal is lower. Raw signals in each time point are very low so it is not clear if this decrease in signal is a consequence of error in fluorescence reading or if it is a real inhibition effect. Used inhibitors should not have an impact on glucuronidation, but additional measurements need to be done to confirm this.

Another CYP3A4 inhibitor, erythromycin, was also tested in the IMER setup under the same conditions. In contrast to ketoconazole, erythromycin is a time-dependent, (mechanism-based) irreversible inhibitor (Zhang *et al.*, 2009). Consequently, it was expected that after an increase

in inhibition in the first two steps of the experiment, where erythromycin concentration was increasing, the amount of metabolite produced would not rise again in the third step (contrary to inhibition with ketoconazole), where the erythromycin concentration was again decreased to 0 μM . This is because erythromycin should still be bound to the enzyme and therefore, still inhibit the metabolism of paclitaxel (CYP1B1 inhibitor), even though there are no new erythromycin molecules fed to the IMER. In this way, it would be immediately visible that erythromycin is a time-dependent (mechanism-based) inhibitor.

However, similar to the inhibition experiment in static conditions (Figure 23), inhibition of BR metabolism by the combination of paclitaxel (inhibits BR metabolism by inhibiting CYP1B1) and erythromycin (inhibits paclitaxel metabolism by inhibiting CYP3A4) did not result in detectable inhibition of BR dealcoxylation suggesting that paclitaxel is effectively metabolized in HIMs also in the presence of erythromycin (CYP3A4 inhibitor) (Figure 26).

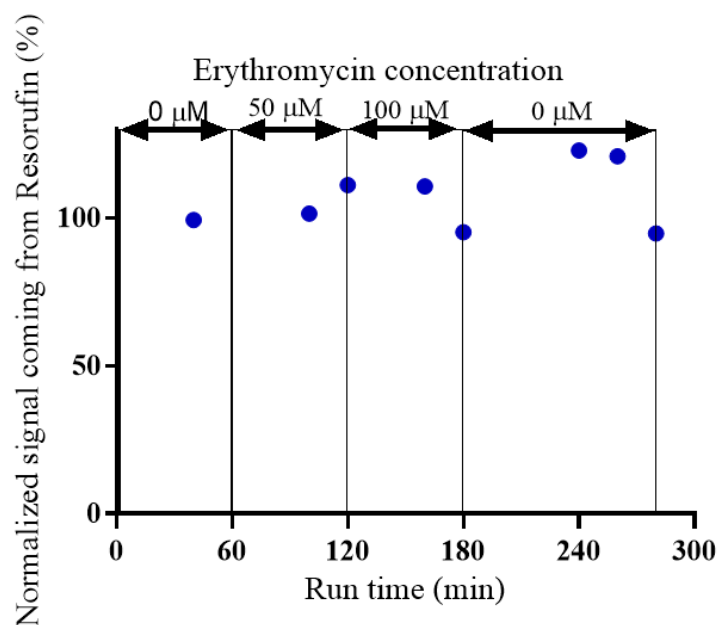


Figure 26. Effect of the increase and decrease of erythromycin concentration on BR transformation incubated with paclitaxel, expressed as an amount of metabolite produced ($N = 2$, $37\text{ }^{\circ}\text{C}$, flow rate: $5.0\text{ }\mu\text{L}/\text{min}$, substrate: $2.0\text{ }\mu\text{M}$ BR, $50.0\text{ }\mu\text{M}$ 8-HQ). Data points on the vertical lines belong to the step prior to the line. N corresponds to the number of replicates.

Possible explanation for these results is that there are other enzymes that contribute to paclitaxel metabolism present in HIM (CYP2C) and reduce its inhibitory potential toward CYP1B1. In contrast to erythromycin, ketoconazole is not selective in high concentrations it inhibits other

enzymes by which paclitaxel could be metabolized, therefore allowing inhibition of CYP1B1 by paclitaxel

The above presented IMER experiments could be translated to a clinical example – co-medication of a cancer patient treated with paclitaxel, who also needs antimicrobial therapy (ketoconazole or erythromycin). The mentioned antimicrobial drugs can increase concentration of the anticancer agent (paclitaxel) to toxic concentrations, where paclitaxel would present its adverse effects. Moreover, increasing paclitaxel concentration above its inhibitory concentration towards CYP1B1 would result in additional adverse effects resulting from CYP1B1 inhibition, which has a critical role in steroid and procarcinogen metabolism. This effect was visible *in vitro* (Figure 24) because concentrations of inhibitors were exaggerated. However, DDI of docetaxel, a similar anticancer agent, and ketoconazole applied in therapeutic concentrations was reported to be clinically insignificant (Engels *et al.*, 2006).

5. CONCLUSION

In this work, a first in its kind microfluidic enzyme reactor with immobilized human intestinal microsomes was developed and evaluated as a platform for intestinal drug-drug interaction research. Goals from the beginning of the work were accomplished:

- First in its kind enzyme reactor with immobilized human intestinal microsomes was developed, with a relatively high immobilization yield and enzyme activity retention of more than 8 hours.
- The developed IMER was shown to be a useful platform for an easy determination of enzyme inhibition mechanism. Furthermore, this device shows a high potential in future experiments of human gut metabolism and, for example, further studies on drug-drug interactions.

Moreover, during a work on this thesis a new piece of scientific information was discovered, showing that:

- It is possible that CYP1B1 is more abundant than previously reported in the literature.
- 7-benzyloxyresorufin in intestinal microsomes is mostly metabolized by CYP1B1.
- An adjustment of previously reported immobilization method resulted in 5-fold more efficient method, which achieves higher final enzyme activities.

On the other hand, some drawbacks were also noticed:

- Not all molecules are suitable for IMER setup.
- There is a high variability between different IMERs.

To summarize, after solving the variability and suitability issues, the developed IMER could serve pharma industry as a good platform for intestinal drug metabolism research, especially for mechanistic determination of enzyme inhibition and drug-drug interactions, due to its high-throughput potential and significant reagents savings.

6. ABBREVIATION LIST

8-HQ – 8-hydroxyquinoline

8-HQ-Glu – 8-hydroxyquinoline-glucuronide

ACN – acetonitrile

AUC – area under the curve

AUCR – area under the curve ratio

b-FL – biotinylated fusogenic liposomes

b-HIM – biotinylated human intestinal microsomes

BR – 7-benzyloxyresorufin

CYP – cytochrome P450

DBF – dibenzylfluorescein

DDI – drug-drug interaction

DMSO – dimethyl sulfoxide

DOPE – 1,2-dioleoyl-*sn*-glycero-3-phosphoethanolamine

DOTAP – 1,2-dioleoyl-3-trimethylammonium-propane

EtOH – ethanol

ER – endoplasmic reticulum

FMO – flavin monooxygenase

LUV – large unilamellar vesicles (liposomes)

HIM – human intestinal microsomes

HLM – human liver microsomes

IC₅₀ – half-maximal inhibitory concentration

IMER – immobilized enzyme (micro)reactor

MeOH – methanol

NADPH – nicotinamide adenine dinucleotide phosphate

OSTE – off-stoichiometry thiol-ene

PBPK model - physiologically based pharmacokinetic model

PBS – phosphate buffer saline

PDMS – polydimethylsiloxane

UDGPA – uridine diphosphate glucuronic acid

UGT – UDP-glucuronosyltransferase

7. REFERENCES

Abgrall P, Conedera V, Camon H, Gue AM, Nguyen NT. SU-8 as a structural material for lab-on-chips and microelectromechanical systems. *Electrophoresis*, 2007, 28(24), 4539-4551.

Becker H, Gärtner C. Polymer microfabrication technologies for microfluidic systems. *Anal Bioanal Chem*, 2008, 390, 89–111.

Bentley P, Oesch F, Glatt H. Dual role of epoxide hydratase in both activation and inactivation of benzo(a)pyrene. *Arch Toxicol*, 1977, 30;39(1-2):65-75.

Brandon EF, Raap CD, Meijerman I, Beijnen JH, Schellens JH. An update on in vitro test methods in human hepatic drug biotransformation research: pros and cons. *Toxicol Appl Pharmacol*, 2003, 189(3):233-246.

Carlborg CF, Haraldsson T, Öberg K, Malkoch M, van der Wijngaart W. Beyond PDMS: off-stoichiometry thiol-ene (OSTE) based soft lithography for rapid prototyping of microfluidic devices. *Lab Chip*, 2011, 21;11(18), 3136-3147.

Chauret N, Gauthier A, Nicoll-Griffith DA. Effect of common organic solvents on in vitro cytochrome P450-mediated metabolic activities in human liver microsomes. *Drug Metab Dispos*, 1998, 26(1), 1-4.

Coleman MD. Human Drug Metabolism: An Introduction, Second Edition. UK, John Wiley & Sons, 2010, 31-32.

Coleman MD. Human Drug Metabolism: An Introduction, Second Edition. UK, John Wiley & Sons, 2010, 97-105.

Continuous flow microfluidics, 2018, https://www.bi-pol.com/microfluidics_chips/, visited 30th January 2022

Datta S, Christena LR, Rajaram YR. Enzyme immobilization: an overview on techniques and support materials. *3 Biotech*, 2013, 3(1), 1-9.

Digital microfluidics, 2016, <https://research2reality.com/health-medicine/shrinking-the-lab/>, visited 30th January 2022

Droplet microfluidics, 2018, <https://www.elveflow.com>, visited 30th January 2022

Engels FK, Mathot RA, Loos WJ, van Schaik RH, Verweij J. Influence of high-dose ketoconazole on the pharmacokinetics of docetaxel. *Cancer Biol Ther*, 2006, 5(7), 833-839.

First pass effect, 2019, <https://www.knowledgedose.com/drugs-undergoing-extensive-first-pass-metabolism/>, visited 30th January 2022

Fisher MB, Paine MF, Strelevitz TJ, Wrighton SA. The role of hepatic and extrahepatic UDP-glucuronosyltransferases in human drug metabolism. *Drug Metab Rev*, 2001, 33(3-4), 273-297.

Fohner AE, Sparreboom A, Altman RB, Klein TE. PharmGKB summary: Macrolide antibiotic pathway, pharmacokinetics/pharmacodynamics. *Pharmacogenet Genomics*, 2017, 27(4), 164-167.

Galetin A, Gertz M, Houston JB. Potential role of intestinal first-pass metabolism in the prediction of drug-drug interactions. *Expert Opin Drug Metab Toxicol*, 2008, 4(7), 909-922.

Greenblatt DJ, Venkatakrishnan K, Harmatz JS, Parent SJ, von Moltke LL. Sources of variability in ketoconazole inhibition of human cytochrome P450 3A in vitro. *Xenobiotica*, 2010, 40(10), 713-720.

Greenblatt DJ, von Moltke LL, Harmatz JS, Counihan M, Graf JA, Durol AL, Mertzanis P, Duan SX, Wright CE, Shader RI. Inhibition of triazolam clearance by macrolide antimicrobial agents: in vitro correlates and dynamic consequences. *Clin Pharmacol Ther*, 1998, 64(3), 278-285.

Guideline on the investigation of drug interactions, 2012, European Medicine Agency, 44.

Gundert-Remy U, Bernauer U, Blömeke B, Döring B, Fabian E, Goebel C, Hessel S, Jäckh C, Lampen A, Oesch F, Petzinger E, Völkel W, Roos PH. Extrahepatic metabolism at the body's internal-external interfaces. *Drug Metab Rev*, 2014, 46(3), 291-324.

Harbourt DE, Fallon JK, Ito S, Baba T, Ritter JK, Glish GL, Smith PC. Quantification of human uridine-diphosphate glucuronosyl transferase 1A isoforms in liver, intestine, and kidney using nanobore liquid chromatography-tandem mass spectrometry. *Anal Chem*, 2012, 84(1), 98-105.

Hassan ME, Yang Q, Xiao Z, Liu L, Wang N, Cui X, Yang L. Impact of immobilization technology in industrial and pharmaceutical applications. *3 Biotech*, 2019, 9(12), 440.

HIM quality certificate, 2020, https://certs-ecatalog.corning.com/life-sciences/certs/452210_9245002.pdf, visited 23rd March 2022.

HLM quality certificate, 2018, https://certs-ecatalog.corning.com/life-sciences/certs/452161_7331001.pdf, visited 23rd March 2022.

In Vitro Drug Interaction Studies - Cytochrome P450 Enzyme and Transporter Mediated Drug Interactions, FDA Guidance, 1(1), pp. 1–46.

Kiiski I. Immobilized Enzyme Microreactors. University of Helsinki, 2021, doctoral thesis.

Kiiski I, Ollikainen E, Artes S, Järvinen P, Jokinen V, Sikanen T. Drug glucuronidation assays on human liver microsomes immobilized on microfluidic flow-through reactors. *Eur J Pharm Sci*, 2021, 158:105677.

Kiiski IMA, Pihlaja T, Urvas L, Witos J, Wiedmer SK, Jokinen VP, Sikanen TM. Overcoming the Pitfalls of Cytochrome P450 Immobilization through the Use of Fusogenic Liposomes. *Adv Biosyst*, 2019, 3(1), e1800245.

Kim JH, Choi WG, Lee S, Lee HS. Revisiting the Metabolism and Bioactivation of Ketoconazole in Human and Mouse Using Liquid Chromatography-Mass Spectrometry-Based Metabolomics. *Int J Mol Sci*, 2017, 18(3), 621.

Li F, Zhu W, Gonzalez FJ. Potential role of CYP1B1 in the development and treatment of metabolic diseases. *Pharmacol Ther*, 2017, 178, 18-30.

Liu Y, Sun L, Zhang H, Shang L, Zhao Y. Microfluidics for Drug Development: From Synthesis to Evaluation. *Chem Rev*, 2021, 121(13), 7468-7529.

Liu Y, Coughtrie MWH. Revisiting the Latency of Uridine Diphosphate-Glucuronosyltransferases (UGTs)-How Does the Endoplasmic Reticulum Membrane Influence Their Function? *Pharmaceutics*, 2017, 9(3):32.

Naritomi Y, Teramura Y, Terashita S, Kagayama A. Utility of microtiter plate assays for human cytochrome P450 inhibition studies in drug discovery: application of simple method for detecting quasi-irreversible and irreversible inhibitors. *Drug Metab Pharmacokinet*, 2004, 19(1), 55-61.

Nicoli R, Bartolini M, Rudaz S, Andrisano V, Veuthey JL. Development of immobilized enzyme reactors based on human recombinant cytochrome P450 enzymes for phase I drug metabolism studies. *J Chromatogr A*, 2008, 1206(1), 2-10.

Paine MF, Hart HL, Ludington SS, Haining RL, Rettie AE, Zeldin DC. The human intestinal cytochrome P450 "pie". *Drug Metab Dispos*, 2006, 34(5), 880-886.

Patabadige DE, Jia S, Sibbitts J, Sadeghi J, Sellens K, Culbertson CT. Micro Total Analysis Systems: Fundamental Advances and Applications. *Anal Chem*, 2016, 88(1), 320-338.

Ren K, Zhou J, Wu H. Materials for microfluidic chip fabrication. *Acc Chem Res*, 2013, 46(11), 2396-2406.

Riches Z, Stanley EL, Bloomer JC, Coughtrie MW. Quantitative evaluation of the expression and activity of five major sulfotransferases (SULTs) in human tissues: the SULT "pie". *Drug Metab Dispos*, 2009, 37(11), 2255-2261.

Rochat B, Morsman JM, Murray GI, Figg WD, McLeod HL. Human CYP1B1 and anticancer agent metabolism: mechanism for tumor-specific drug inactivation? *J Pharmacol Exp Ther*, 2001, 296(2), 537-541.

Schejbal J, Řemínek R, Zeman L, Mádr A, Glatz Z. On-line coupling of immobilized cytochrome P450 microreactor and capillary electrophoresis: A promising tool for drug development. *J Chromatogr A*, 2016, 11,1437, 234-240.

Sheldon RA, van Pelt S. Enzyme immobilisation in biocatalysis: why, what and how. *Chem Soc Rev*, 2013, 42(15), 6223-6235.

Sikanen MT, Lafleur JP, Moilanen ME, Zhuang G, Jensen TG, Kutter JP. Fabrication and bonding of thiol-ene-based microfluidic devices. *J Micromech Microeng*, 2013, 23, 037002.

Spratlin J, Sawyer MB. Pharmacogenetics of paclitaxel metabolism. *Crit Rev Oncol Hematol*, 2007, 61(3), 222-229.

Stresser DM, Turner SD, Blanchard AP, Miller VP, Crespi CL. Cytochrome P450 fluorometric substrates: identification of isoform-selective probes for rat CYP2D2 and human CYP3A4. *Drug Metab Dispos*, 2002, 30(7), 845-852.

Tähkä S, Sarfraz J, Urvas L, Provenzani R, Wiedmer KS, Peltonen J, Jokinen V, Sikanen T. Immobilization of proteolytic enzymes on replica-molded thiol-ene micropillar reactors via thiol-gold interaction. *Anal Bioanal Chem*, 2019, 411, 2339–2349.

Thelen K, Dressman JB. Cytochrome P450-mediated metabolism in the human gut wall. *J Pharm Pharmacol*, 2009, 61(5), 541-558.

Whitesides GM. The origins and the future of microfluidics. *Nature*, 2006, 442(7101), 368-373.

Wienkers L, Heath T. Predicting in vivo drug interactions from in vitro drug discovery data. *Nat Rev Drug Discov*, 2005, 4, 825–833.

Wu Q, Liu J, Wang X, Feng L, Wu J, Zhu X, Wen W, Gong X. Organ-on-a-chip: recent breakthroughs and future prospects. *Biomed Eng Online*, 2020, 19(1), 9.

Xia Y, Whitesides GM. Soft Lithography. *Angew Chem Int Ed Engl*, 1998, 6;37(5):550-575.

Yamada M, Inoue SI, Sugiyama D, Nishiya Y, Ishizuka T, Watanabe A, Watanabe K, Yamashita S, Watanabe N. Critical Impact of Drug-Drug Interactions via Intestinal CYP3A in the Risk Assessment of Weak Perpetrators Using Physiologically Based Pharmacokinetic Models. *Drug Metab Dispos*, 2020, 48(4),288-296.

Zhang QY, Dunbar D, Ostrowska A, Zeisloft S, Yang J, Kaminsky LS. Characterization of human small intestinal cytochromes P-450. *Drug Metab Dispos*, 1999, 27(7), 804-809.

8. SUMMARY

Human intestinal metabolism is emerging to be more important than what was previously thought, especially in pharma industry when the inhibitory potential of a new drug candidate is being determined. It was shown that intestinal metabolism has a critical role in determining a need for clinical drug-drug interaction studies for weak CYP3A perpetrators.

On the other hand, conventional static *in vitro* enzymatic assays demand a high consumption of enzymes and other chemicals, the separation step is always needed before product detection, and without flow-through conditions, there are limitations in imitating conditions in human body.

In this work, the first in its kind immobilized enzyme microreactor (IMER) was developed by using human-derived intestinal microsomes and characterized in the terms of enzyme immobilization yield and stability of enzyme activity. The microreactor was made from off-stoichiometric thiol-enes and microsomes were immobilized by fusion with previously immobilized biotinylated fusogenic liposomes being held in place *via* biotin-streptavidin interaction.

A full potential of this platform was shown by enzyme inhibition mechanism determination, with performing only one experiment where feed solution containing different inhibitor concentrations in different time points was passing through the microreactor

In addition, it was shown that CYP1B1 could be more expressed in HIM than it was previously reported.

SAŽETAK

Intestinalni metabolizam u ljudi sve više pridobiva na važnosti, pogotovo u farmaceutskoj industriji kada se određuje inhibitorni potencijal novih lijekova kandidata. Pokazano je da intestinalni metabolizam ima ključnu ulogu u određivanju potrebe za kliničkim lijek-lijek interakcija studijama za slabe CYP3A inhibitore.

Konvencionalni statički in vitro enzimatski eksperimenti zahtijevaju velik utrošak kemikalija pa tako i skupih kofaktora i enzima, prije detekcije potreban je korak odijeljivanja produkta, a bez prisutnosti protoka značajnija imitacija uvjeta ljudskog organizma nije ostvarena.

U ovom radu razvijen je mikrofluidički imobilizirani enzimatski reaktor s imobiliziranim humanim intestinalnim mikrosomima te je okarakteriziran u pogledu stabilnosti enzimatske aktivnosti. Mikroreaktor je napravljen on tiol-ena u nestehiometrijskom omjeru, a mikrosomi su imobilizirani fuzijom mikrosoma s prethodnom imobiliziranim liposomima, koji su vezani biotin-streptavidin interakcijom.

Puni potencijal ove platforme pokazan je određivanjem mehanizma enzimatske inhibicije samo jednim eksperimentom u kojem supstrati reakcije teku preko imobiliziranih enzima u različitim koncentracijama tijekom eksperimenta.

Također, pokazano je da bi CYP1B1 mogao biti više eksprimiran u humanim intestinalnim mikrosomima nego što je ranije bilo pokazano.

9. ATTACHMENTS

9.1. Information About Enzyme Source from the Supplier

9.1.1. HIM

- Producer: Corning
- LOT: 9245002
- Date released: February 2020
- Pool is comprised of five donor specimens
- Protein content: 10 mg/mL in 10 mM sucrose, 10 mM KPO₄, 1 mM EDTA, pH 7.4

Table 11. HIM assay results (quality certificate taken from supplier, taken from: https://certs-ecatalog.corning.com/life-sciences/certs/452210_9245002.pdf).

Enzyme Measured	Assay	Enzyme Activity [in pmol/(mg x min)]
OR	Cytochrome c Reductase	99
CYP2C9	Diclofenac 4'-Hydroxylase	130
CYP3A4	Testosterone 6 β -Hydroxylase	3000
CYP2J2/4F12	Astemizole O-Demethylase	59
UGT1A1/8/10	Estradiol 3-Glucuronidation	10000
Carboxylesterase (hCE1/2)	<i>para</i> -Nitrophenylacetate Hydrolase	3200

- Pool is comprised of donor specimens 23355, 3210602, 3225745, 3226923, and 3262887. The microsomes were prepared from both duodenum and jejunum sections. Only mature enterocytes, which are enriched in P450 and UGT activity, were used in the microsome preparation. Enterocyte isolation was based on the elution method (Drug Metab. Dispos. 27: 804-809, 1999). Intestine cold ischemic time (time prior to cell harvest) was less than 24 hours.
- All cytochrome P450 assays conducted at 0.8 mg/ml protein (except CYP2J2/4F12 which was at 1 mg/ml) with an NADPH generating system (1.3 mM NADP, 3.3 mM glucose 6-phosphate and 0.4 U/ml glucose 6-phosphate dehydrogenase), 3.3 mM MgCl₂, and incubated for 10 mins for CYP3A4 assay, and 30 mins for CYP2J2/4F12 and CYP2C9 assays. 0.1 M Potassium phosphate buffer (pH 7.4) was used for all P450 enzymes except CYP2C9, which used 0.1 M Tris (pH 7.5).
- UGT Glucuronidation assays contained 0.1 mg/ml protein, 2 mM UDPGA, 10 mM MgCl₂, 25 ug/ml alamethicin in 50 mM Tris-HCl buffer (pH 7.5) and incubated for 20 minutes.
- The enzymatic hydrolysis of p-nitrophenylacetate was followed spectrophotometrically at 400 nm for one minute. Incubations contained 0.016 mg/ml protein in 0.1 M potassium phosphate buffer (pH 7.4). The reported activity was found to be comparable to the activity observed in pooled HLM (Cat# 452161) in a side-by-side comparison study.
- Enzyme activities are expressed as pmole product per (mg protein x minute) except cytochrome c reductase and p-nitrophenylacetate hydrolase, which are expressed as nmol product per (mg protein X minute).
- The effect of repeated freeze/thaw cycles was tested for each enzyme activity. Minimal loss was observed (less than 10%) after 6 freeze/thaw cycles. We recommend aliquoting to minimize the number of freeze/thaw cycles.

9.1.2. HLM

- Producer: Corning
- LOT: 7331001
- Date released: April 2018
- Pool is comprised of 26 donor specimens
- Protein content: 20 mg/mL in 250 mM sucrose

Table 12. HLM assay results (quality certificate taken from supplier, adapted from: https://certs-ecatalog.corning.com/life-sciences/certs/452161_7331001.pdf).

Enzyme Measured	Assay	Enzyme Activity [in pmol/(mg x min)]
Total P450	Omura and Sato	360 pmol/mg
OR	Cytochrome c Reductase	260 nmol/(mg x min)
Cytochrome b ₅	Spectrophotometric	540 pmol/mg
CYP1A2	Phenacetin O-deethylase	830
CYP2A6	Coumarin 7-hydroxylase	870
CYP2B6	Bupropion hydroxylase	380
CYP2C8	Paclitaxel 6 α -hydroxylase	330
CYP2C9	Diclofenac 4'-hydroxylase	3000
CYP2C19	(S)-Mephenytoin 4'-hydroxylase	54
CYP2D6	Bufuralol 1'-hydroxylase (The amount of activity inhibited by 1 μ M quinidine.)	240
CYP2E1	Chlorzoxazone 6-hydroxylase	2700
CYP3A4	Testosterone 6 β -hydroxylase	3400
CYP4A11	Lauric acid 12-hydroxylase	1400
FMO	Methyl p-Tolyl Sulfide Oxidase	1500
UGT1A1	Estradiol 3-Glucuronidation	1300
UGT1A4	Trifluoperazine N-Glucuronidation	710
UGT1A9	Propofol Glucuronidation	4700

- Pool is comprised of HMC85G, HFC165, HFC173, HMC184, HFC195, HMC207, HMAA213, HMC506, HMC524, HMC557, HFC56, HMC572, HMC577, HMC582, HMC628, HMC635, HMC64, HMC661, HMC673, HMC689, HFC692, HFC759, HFC804, HMC822, HFC824, and HMC855
- All cytochrome P450 assays were conducted at 0.8 mg/mL protein (except CYP2B6 which was at 0.1 mg/mL, CYP2C19 which was at 0.3 mg/mL, and CYP3A4 which was at 0.5 mg/mL) with an NADPH generating system (1.3 mM NADP, 3.3 mM glucose 6-phosphate, 3.3 mM MgCl₂, and 0.4 U/mL glucose 6-phosphate dehydrogenase) and incubated for 20 minutes (except CYP2B6 which was incubated for 5 minutes and CYP2C8, CYP2C9, CYP2C19, CYP3A4 and CYP4A11 which were incubated for 10 minutes). 0.1 M Potassium phosphate buffer, pH 7.4 was used for all P450 enzymes (except 0.5 M Potassium phosphate buffer, pH 9.4 was used for CYP2B6 and CYP2C19 and 0.1 M Tris buffer, pH 9.5 was used for CYP2A6, CYP2C9 and CYP4A11). The FMO assay was conducted at 0.8 mg/mL protein with a NADPH generating system, 1.2 mM diethylenetriaminepentacetic acid, 0.5 mg/mL Triton X-100 in 0.05 M glycine buffer, pH 9.5 and was incubated for 10 minutes. All UGT Glucuronidation assays were conducted at 0.5 mg/mL protein (except UGT1A9 which was at 0.15 mg/mL), 2 mM UDPGA, 10 mM MgCl₂, 25 μ g/mL Alamethicin in 0.1 M Tris buffer, pH 9.5. UGT1A1 was incubated for 30 minutes, UGT1A4 for 20 minutes, and UGT1A9 for 10 minutes. Activities expressed as pmol product per mg protein x minute (except cytochrome c reductase which is expressed as nmole product per mg protein x minute).

CURRICULUM VITAE

Research experience:

(May 2022 – Sep 2022)	Freie Universität Berlin <ul style="list-style-type: none">– Pharmacometrics
Mar 2021 – Jul 2021	University of Helsinki <ul style="list-style-type: none">– Microfluidic immobilized enzyme microreactor for intestinal drug metabolism research
Nov 2020 – Feb 2021	Xellia Pharmaceuticals <ul style="list-style-type: none">– Preparation and characterization of glycopeptide-loaded liposomes
Jun 2019 – Sep 2019	University of Cambridge <ul style="list-style-type: none">– Identifying novel PARP inhibitors by <i>in silico</i> screening and <i>in vitro</i> testing
Sep 2017 – Sep 2018	University of Zagreb <ul style="list-style-type: none">– Kinetics and mechanism of activation of C – H bond in azobenzenes by Pd(II) catalyst

Other experience:

Sep 2020 –	Top Matura <ul style="list-style-type: none">– Chemistry teacher
Sep 2020 – Sep 2021	International Pharmaceutical Students' Federation (IPSF) <ul style="list-style-type: none">– Pharmaceutical Sciences Coordinator
Oct 2019 – Oct 2021	University of Zagreb <ul style="list-style-type: none">– Deputy member of Students' Council
Jan 2019 – Jun 2109	International Society for Applied Biological Sciences (ISABS) <ul style="list-style-type: none">– Organizing committee of the 11th ISABS Conference and Mayo Clinic Lectures in Individualized Medicine
Oct 2018 – Oct 2019	Croatian Pharmaceutical Students' Association (CPSA) <ul style="list-style-type: none">– Chairperson of the 6th CPSA Congress– Organizing committee of the Clinical Skills Event– Organizing committee of the 5th CPSA Congress
Jan 2018 – May 2018	
Oct 2017 – Oct 2018	
Sep 2019 – Oct 2019	European Pharmaceutical Students' Association (EPSA) <ul style="list-style-type: none">– Helping committee of the 16th EPSA Autumn Assembly– Official delegate for Croatia– National Twinnet coordinator
Oct 2017 – Oct 2019	
Oct 2017 – Oct 2019	
Oct 2017 – Mar 2018	Faculty of Pharmacy and Biochemistry, Department of Biophysics <ul style="list-style-type: none">– Student assistant

Education:

Oct 2016 – (Apr 2022)	Faculty of Pharmacy and Biochemistry, University of Zagreb <ul style="list-style-type: none">– Average grade: 4.5 / 5.0– Sport association – volleyball– CPSA– Choir <i>Cappella Panacea</i>
2020	*Dean's acknowledgment – the best student on the year based on grades (average grade on 4th y: 5.00)
2019	*Dean's award – Kinetics and Mechanism of cyclopalladation of 4-Dimethyl Azobenzenes

Short students' exchanges:

2019	Charles University, Prague
2019	Marmara University, Istanbul
2018	Aix-Marseille University, Marseille
2019	University of Graz, Graz

Articles:

- Bjelopetrović A, Barišić D, Duvnjak Z, Džajić I, Kulcsár MJ, Halasz I, Martinez M, Budimir A, Babić D, Ćurić M. **A Detailed Kinetic-Mechanistic Investigation on the Palladium C–H Bond Activation in Azobenzenes and Their Mono-palladated Derivatives.** *Inorganic Chemistry*. 2020 Nov
- Mlinarić, Z., Duvnjak, Z., Fajdetic, A., Gavran, L., Kučević, A., Kuvek, T., Levatić, M., Bojić, M. (2021). **The effect of selected xenobiotics on the urine colour.** *Farmaceutski glasnik 77*, 5-6/2021, review article
- Duvnjak, Z., Gutierrez, M.E., Greenhalgh, J.C., Robinson, J., Rahman, T. (2020). **Identifying novel naturally-occurring chemical scaffolds as potential inhibitors of Poly(ADP-ribose) polymer-ase (PARP).** *EPSA Students' Science Publication, volume 8*
- Duvnjak, Z., Božičević, L. (2019). **6th Croatian Pharmacy and Medical Biochemistry Students' Association's Congress.** *Farmaceutski glasnik 75*, 7-8/2019

Oral presentations:

- Duvnjak, Z. (2021). **Microfluidic Immobilized Enzyme Microreactor for Intestinal Drug Metabolism Research.** *9th Pharmacy and Medicinal Biochemistry Student Symposium*. Zagreb: Faculty of Pharmacy and Biochemistry
- *award for the best oral presentation

Poster presentations:

- Duvnjak, Z., Ekwere Williams, A., Yahya, S., Fouaad M., Sham, T.T. (2020). **The Assessment of Pharmacy Students Involvement in Scientific Research Projects.** *FIP World Congress 2020, online event*

Duvnjak, Z., Gutierrez, M.E., Greenhalgh, J.C., Robinson, J., Rahman, T. (2019). **Identifying novel naturally-occurring chemical scaffolds as potential inhibitors of Poly(ADP-ribose) polymer-ase (PARP)**. *Pharmacology Away Day 2019* (pp.19), University of Cambridge, UK
*award for the best poster presentation

Duvnjak, Z., et al. (2019). **Effect of Temperature on Dicyclopalladation of 4-dimethylaminoazobenzenes**. In N. Galić & M. Rogošić; *26th Croatian Meeting of Chemists and Chemical Engineers with international participation* (pp. 59).

Džajić, I., Duvnjak, Z., et al. (2019) **Kinetics and Mechanism of the Second Palladation of Monopalladated Azobenzenes**. *42nd European Pharmaceutical Students' Association's Annual Congress*, Sofia, Bulgaria

Begović, I., Belec, D., Beljan, A., Benković, A., Bulović, E., Čurt, E., Durbek, J., Duvnjak, Z., Dužević, M., Grabić, M., Kurija, J., Mahovlić, L., Milardović, M., Miljak, K., Mitrović, I., Mrše, A., Parac, P., Pejaković, T.I., Rački, B., Šarenić, P., Šipicki, S., Šojat, M., Tešić, D., Tešija, L., Tićak, B., Tomašić, L., Tušinec, M., Vađunec, D., Žili, K., Žunić, K. (2018) **#BreakTheStigma**. In M. Bojić & P. Turčić, *7th Pharmacy and Medicinal Biochemistry Student Symposium* (pp. 17). Zagreb: Faculty of Pharmacy and Biochemistry.

Duvnjak, Z., Džajić, I., Budimir, A., Juribašić Kulcsar, M. & Čurić, M. (2018). **Kinetics of Cyclopalladation of Methyl Orange with Bis(acetonitrile)dichloropalladium(II)**. In M. Bojić & P. Turčić, *7th Pharmacy and Medicinal Biochemistry Student Symposium* (pp. 35). Zagreb: Faculty of Pharmacy and Biochemistry.

Temeljna dokumentacijska kartica

Sveučilište u Zagrebu
Farmaceutsko-biokemijski fakultet
Studij: Farmacija
Zavod za farmaceutsku kemiju
A. Kovačića 1, 10000 Zagreb, Hrvatska

Diplomski rad

Mikrofluidički enzimatski reaktor s imobiliziranim humanim intestinalnim mikrosomima

Zrinka Duvnjak

SAŽETAK

Intestinalni metabolizam u ljudi sve više pridobiva na važnosti, pogotovo u farmaceutskoj industriji kada se određuje inhibitorski potencijal novih lijekova kandidata. Pokazano je da intestinalni metabolizam ima ključnu ulogu u određivanju potrebe za kliničkim lijek-lijek interakcijama za slabe CYP3A inhibitore.

Konvencionalni statički *in vitro* enzimatski eksperimenti zahtijevaju velik utrošak kemikalija pa tako i skupih kofaktora i enzima, prije detekcije potreban je korak odijeljivanja produkta, a bez prisutnosti protoka značajnija imitacija uvjeta ljudskog organizma nije ostvarena.

U ovom radu razvijen je mikrofluidički imobilizirani enzimatski reaktor s imobiliziranim humanim intestinalnim mikrosomima te je okarakteriziran u pogledu stabilnosti enzimatske aktivnosti. Mikroreaktor je napravljen od tiol-ena u nestehiometrijskom omjeru, a mikrosomi su imobilizirani fuzijom mikrosoma s prethodnom imobiliziranim liposomima, koji su vezani biotin-streptavidin interakcijom.

Puni potencijal ove platforme pokazan je određivanjem mehanizma enzimatske inhibicije samo jednim eksperimentom u kojem supstrati reakcije teku preko imobiliziranih enzima u različitim koncentracijama tijekom eksperimenta.

Također, pokazano je i da bi CYP1B1 mogao biti više eksprimiran u humanim intestinalnim mikrosomima nego što je ranije bilo pokazano.

Rad je pohranjen u Središnjoj knjižnici Sveučilišta u Zagrebu Farmaceutsko-biokemijskog fakulteta.

Rad sadrži: 58 stranica, 26 grafičkih prikaza, 12 tablica i 53 literaturnih navoda. Izvornik je na engleskom jeziku.

Ključne riječi: *IMER, mikrofluidika, imobilizacija, intestinalni metabolizam, CYP1B1*

Mentori: **Dr. sc. Tiina Sikanen**, *izvanredni profesor Sveučilišta u Helsinkiju, Farmaceutskog fakulteta.*

Dr. sc. Hrvoje Rimac, *docent Sveučilišta u Zagrebu Farmaceutsko-biokemijskog fakulteta.*

Ocjenjivači: **Dr. sc. Hrvoje Rimac**, *docent Sveučilišta u Zagrebu Farmaceutsko-biokemijskog fakulteta.*
Dr. sc. Ana Budimir, *izvanredni profesor Sveučilišta u Zagrebu Farmaceutsko-biokemijskog fakulteta.*

Dr. sc. Zrinka Rajić, *redoviti profesor Sveučilišta u Zagrebu Farmaceutsko-biokemijskog fakulteta.*

Rad prihvaćen: travanj 2022.

Basic documentation card

University of Zagreb
Faculty of Pharmacy and Biochemistry
Study: Pharmacy
Department of Medicinal Chemistry
A. Kovačića 1, 10000 Zagreb, Croatia

Diploma thesis

Microfluidic Enzyme Reactor with Immobilized Human Intestinal Microsomes

Zrinka Duvnjak

SUMMARY

Human intestinal metabolism is emerging to be more important than what was previously thought, especially in pharma industry when the inhibitory potential of a new drug candidate is being determined. It was shown that intestinal metabolism has a critical role in determining a need for clinical drug-drug interaction studies for weak CYP3A perpetrators.

On the other hand, conventional static in vitro enzymatic assays demand a high consumption of enzymes and other chemicals, the separation step is always needed before product detection, and without flow-through conditions, there are limitations in imitating conditions in human body.

In this work, the first in its kind immobilized enzyme microreactor (IMER) was developed by using human-derived intestinal microsomes and characterized in the terms of enzyme immobilization yield and stability of enzyme activity. The microreactor was made from off-stoichiometric thiol-enes and microsomes were immobilized by fusion with previously immobilized biotinylated fusogenic liposomes being held in place via biotin-streptavidin interaction.

A full potential of this platform was shown by enzyme inhibition mechanism determination, with performing only one experiment where feed solution containing different inhibitor concentrations in different time points was passing through the microreactor

In addition, it was shown that CYP1B1 could be more expressed in HIM than it was previously reported.

The thesis is deposited in the Central Library of the University of Zagreb Faculty of Pharmacy and Biochemistry.

Thesis includes: 58 pages, 26 figures, 12 tables and 53 references. Original is in English language.

Keywords: *IMER, microfluidics, immobilization, intestinal metabolism, CYP1B1*

Mentors: **Tiina Sikanen, Ph.D.**, Associate Professor, University of Helsinki, Faculty of Pharmacy
Hrvoje Rimac, Ph.D., Assistant Professor, University of Zagreb, Faculty of Pharmacy and Biochemistry

Reviewers: **Hrvoje Rimac, Ph.D.**, Assistant Professor, University of Zagreb, Faculty of Pharmacy and Biochemistry
Ana Budimir, Ph.D., Associate Professor, University of Zagreb, Faculty of Pharmacy and Biochemistry
Zrinka Rajić, Ph.D., Full Professor, University of Zagreb, Faculty of Pharmacy and Biochemistry

The thesis was accepted: April 2022.